1-1-2013

Real Time Estimation, Quantization, And Remote Control Of Permanent Magnet Dc Motors

Mohammad Obeidat
Wayne State University,

REAL TIME ESTIMATION, QUANTIZATION, AND REMOTE CONTROL OF PERMANENT MAGNET DC MOTORS

by

MOHAMMAD ALI AHMED OBEIDAT

DISSERTATION

Submitted to the Graduate School

of Wayne State University,

Detroit, Michigan

in partial fulfillment of the requirements

for the degree of

DOCTOR OF PHILOSOPHY

2013

MAJOR: ELECTRICAL ENGINEERING

Approved by:

_____

Adviser Date

_____

_____

_____

_____

DEDICATION

To my Parents

my Wife

my Kids Nada, Alfudel, Redda, and Myar

and all my family

ACKNOWLEDGEMENT

In The Name of Allah, The Most Beneficent, The Most Merciful. First, I want to thank allah for reaching this situation and getting my PhD in Electrical Engineering.

Second, There are several people who deserve my heartfelt thanks for their generous contributions and support to this dissertation. I would like to express my sincere appreciation to Professor Le Yi Wang, who contributed tremendous time to my research. Without his direction, suggestion, supervision, support, and guidance, I do not believe this dissertation would have been completed. Appreciation is also due to Professor Feng Lin, Professor Abhilash Pandya, Professor Caisheng Wang, and Professor Wen Chen for their constructive comments and valuable suggestions.

The work described in this thesis would not have been possible without the generous financial support from the Tafila Technical Univesity (TTU), Wayne State University (Thomas C.Rumble University Graduate Fellowship and Summer Dissertation Fellowship), and Prof Le Yi Wang (Graduate Research Assistantship).

Furthermore I would also like to acknowledge with much appreciation my mother, my wife, my brothers and sisters for their moral support and encouragement. My lovely kids, Nada, Alfudel, Redda, and Myar also deserve a lot of appreciation for their patience and support. Also special thanks to my uncle Mohammad for his encouragement and support. Many thanks also to all relatives who supported me during my study. Finally, I would like to thank all my friends in Michigan/USA and Jordan.

TABLE OF CONTENTS

Dedication ii

Acknowledgement iii

List of Tables viii

List of Figures x

Chapter 1 Introduction 1

1.1 Objective and Motivation 2

1.2 Literature Survey 5

1.3 Original Contributions 8

Chapter 2 Background 12

2.1 PMDC Motors 12

2.1.1 Direct Current Motors 12

2.1.2 Permanent Magnet Direct Current Motor (PMDC) 16

2.2 Speed Sensors 17

2.3 System Identification and Parameter Estimation 19

2.4 System Identification with Quantized Observations 23

2.5 Signal Estimation 26

2.5.1 Weighted Empirical Measures 26

2.5.2 Algorithms and Convergence 29

2.6 Control Theory 31
2.6.1 Digital PID Controller 35
2.6.2 Response Performance of Output Signal 38

Chapter 3 Models of PMDC Motors 42

3.1 Continuous-Time PMDC Models 42
3.2 Discretization of PMDC Models 44
3.3 Regression Models 46

Chapter 4 Parameter Estimation of PMDC Motors Using Quantized Sensors 48

4.1 Problem Formulation on Quantized Identification of PMDC Motor Parameters 49
4.2 Binary Identification of PMDC Motors 51
4.2.1 Observation Structures 51
4.2.2 Identification Algorithms 52
4.2.3 Convergence Analysis 54
4.2.4 Examples 55
4.2.5 Threshold Adaptation 59
4.3 Quantized Identification Algorithms 61
4.3.1 Optimal Quasi-Convex Combination Estimator 61
4.3.2 Examples 65
4.4 Experimental Verification 69

Chapter 5 Signal Estimation and Closed-Loop System Performance of PMDC Motors with Communication Channels 73

5.1 Feedback Systems with Communication Channels 75

5.2 Communication Channels and Signal Estimation 80

5.2.1 PMDC Signal Estimation 82

5.2.2 Filter Representation and Error Analysis 84

5.2.3 Impact of Signal Estimation on Feedback Performance 86

5.3 Case Study 1: Output Communication Block 1 Only 89

5.3.1 Impact of Signal Averaging Weight α_1 90

5.3.2 Impact of Sampling Interval T_{s1} 93

5.3.3 Impact on Noise Attenuation 96

5.4 Case Study 2: Both Input and Output Communication Blocks 99

5.4.1 Impact of Signal Averaging Weights α_1 and α_2 99

5.4.2 Impact of Sampling Intervals T_{s1} and T_{s2} 103

5.4.3 Impact of Transmission Errors and Packet Losses 107

5.4.4 Impact of Communication Delays 111

Chapter 6 Conclusion And Future Work 112

6.1 Conclusion 112

6.2 Future Work 113

Refrences 119

Abstract 132

Autobiographical Statement **134**

LIST OF TABLES

Table 1 Parameter Estimation with $M = 240$ V, $\sigma = 4$, and $C = 125$. 56

Table 2 Parameter Estimation $M = 240$ V, $N = 20000$, and $C = 125$. 57

Table 3 Parameter Estimation with $N = 20000$ and $\sigma = 4$ 59

Table 4 Parameter Estimation by Using The Data of Example 5 65

Table 5 Parameter Estimation by Using the Optimal QCCE of 4-Thresholds 66

Table 6 QCCE Estimation Using the Experimental Data of Example 7 72

Table 7 Step Response Performance of Figure 25 91

Table 8 Step Response Performance of Figure 28 94

Table 9 Step Response Performance of Figure 34 100

Table 10 Step Response Performance of Figure 37 102

Table 11 Step Response Performance of Figure 38 104

Table 12 Step Response Performance of Figure 41 106

LIST OF FIGURES

Figure 1 *Schematic Diagram of DC Motor* 14

Figure 2 *Brushed DC Motor Types* 15

Figure 3 *Functions of a Hall Effect Sensor* 20

Figure 4 *System Identification and Parameter Estimation* 22

Figure 5 *PID Controller Block Diagram* 36

Figure 6 *Step Response with Performance Measure Times* 40

Figure 7 *Continuous-time and discrete-time speed of the PMDC motor* . . 45

Figure 8 *Quantized system identification configuration* 50

Figure 9 *The motor speed trajectories using actual and estimated parameters* 57

Figure 10 *Threshold adaptation flowchart* 60

Figure 11 *Speeds of the PMDC motor* 66

Figure 12 *Convergence of the QCCE and convergence rates* 67

Figure 13 *Sample variance of the QCCE estimator vs. the CR lower bound* . 67

Figure 14 *The motor control and evaluation kit* 70

Figure 15 *The experimental verification system* 70

Figure 16 *Periodic input voltage profiles* 71

Figure 17 *Periodic output speeds of the PMDC motor* 72

Figure 18 *Sample variance trajectory of the QCCE estimator vs the CR bound* 73

Figure 19 *Step response of PMDC motor in open loop (without the controller)* 77

Figure 20 *Step response of PMDC motor in closed loop (with the controller)* 77

Figure 21 *Ramp response of the closed-loop system with the PI controller* . . 78

Figure 22 *Sinusoid response of the closed-loop system with the PI controller* . 78

Figure 23 *Closed-loop PMDC system with communication channels* 79

Figure 24 *Simplified equivalent system* 84

Figure 25 *Effects of signal averaging weights: step response* 90

Figure 26 *Effects of signal averaging weights: ramp response* 92

Figure 27 *Effects of signal averaging weights: sinusoid response* 92

Figure 28 *Effects of sampling intervals: step response* 95

Figure 29 *Effects of sampling rates: ramp response* 95

Figure 30 *Effects of sampling rates: sinusoid response* 96

Figure 31 *Effects of noise: step response* 97

Figure 32 *Effects of sampling rates: ramp response* 98

Figure 33 *Effects of sampling rates: sinusoid response* 98

Figure 34 *Effect of signal averaging weights: step response* 100

Figure 35 *Effect of signal averaging weights: ramp response* 101

Figure 36 *Effect of signal averaging weights: sinusoid response* 101

Figure 37 *Effects of different signal averaging on closed loop using two blocks* 102

Figure 38 *Effects of sampling intervals: step response* 103

Figure 39 *Effects of sampling rates: ramp response* 105

Figure 40 *Effects of sampling rates: sinusoid response* 105

Figure 41 *Effects of different sampling rates on closed loop using two blocks* . 106

Figure 42 *Hardware implementation of real time estimation of PMDC parameters* 115

CHAPTER 1: INTRODUCTION

This thesis introduces new methodologies for real-time control-oriented identification of electric machines using quantized sensor information. It employs Permanent Magnet DC Motor (PMDC) motors as a benchmark platform to develop these methods. In this research, several problems of PMDC motors such as modeling, estimation, quantization, and wireless control were investigated. Control theory, system identification, and signal processing technologies are used to solve these problems properly. A closed loop system with communication channels were build to control the speed of PMDC motors through transmitting and receiving the in/out data.

System identification and parameter estimation in dynamic models is of importance for many fields of science and engineering because many physical, chemical and biological processes are described by systems of differential equations with unknown parameters.

System identification and parameter estimation is very important area of research in engineering. In this area the statistical methods are used to build mathematical models of dynamical systems from measured data. The optimal design of experiments is included in system identification to generate informative data that can be used efficiently in a system. In addition to dynamical behavior of the system; for automatic control, these models require important simplifications if the model is to be used in a real-time application. There are different models that can be used to describe the system such as physical, mathematical, mental, statistical, psychological, etc.

Recently, the use of wireless communications in automotive systems to replace wired systems is increased. Many automotive manufacturers are seeking wireless solutions for intra-vehicle control systems. More importantly, in networked systems such as unmanned aerial vehicles, mobile sensor teams, autonomous highway vehicle platoons, wireless communication channels become an integral part of the feedback loop. Introduction of communication channels mandates signal sampling, quantization, and estimation, and consequently adds new dynamic subsystems into the feedback loop. Design variables for the communication systems such as sampling schemes and quantization levels, for signal estimation such as parameter updating step sizes, and controllers such as controller gains, interact and jointly affect feedback performance. This dissertation investigates impact of these design variables and derives some essential guidelines in designing remotely controlled electric motors.

1.1 Objective and Motivation

The main objectives of this dissertation are:

- This dissertation introduces new methodologies for real-time control-oriented identification of electric machines using quantized sensor information. While this methodologies have been mathematically developed with some appealing convergence properties, they have never been applied to system identification of electric machines. This dissertation employs PMDC motors as a benchmark platform to develop our methods. Using binary or quantized sensors is challenging for system modeling, identification and control since they are nonlinear,

discontinuous, and provide very limited information.

Advantages of binary sensors:

- Less complexity
- More cost effective
- Communication channels can be used in remote control real time applications.

- This thesis proposes threshold adaptation technique in parameter estimation process. This technique is useful in increasing the accuracy of the parameter estimation and decreasing the total square error between the estimated and actual parameters. Threshold adaptation depends on accumulative distribution function F(.), the highest slope is near the probability value $\zeta = 0.5$, so threshold value can be chosen according to this.

- This thesis investigates unique issues rising from feedback control of electric motors with embedded communication channels. For concreteness, PMDC motors are employed as a representative system for carrying out our analysis and simulation, although the findings of this dissertation are applicable to other motor types. Adding two embedded communication channels among the feedback is a challenging problem because this will affect the performance of the output response of feedback PMDC systems. Introduction of communication channels adds new dynamic subsystems into the feedback loop. Design variables for the communication systems such as sampling schemes and quantiza-

tion levels, which are directly linked to their resource consumptions, interact with controllers to jointly affect feedback stability and performance. In this thesis the impact of communication strategies on motor feedback systems and the important guidelines in designing remotely controlled electric motors are introduced.

- This dissertation proposes wireless solutions for many automotive systems such as intra-vehicle control systems. More importantly, in networked systems such as unmanned aerial vehicles, mobile sensor teams, autonomous highway vehicle platoons, wireless communication channels become an integral part of the feedback loop.

1.2 Literature Survey

This subsection presents a comprehensive review on existing methodologies in the field of parameter estimation and system identification for electric machines.

The traditional system identification methods, such as least squares, instrumental variables, stochastic approximation, frequency-domain, and maximum likelihood methods use a linear sensor in measuring the output. So the estimation algorithms depend on the calculation of the system output directly. Also many algorithms were developed in system identification and parameter estimation such as algorithms of gradient or Gauss-Newton type. The gradient method has problems when the derivative is used near the switching points. As a result, algorithm for recursive identification of linear systems, using quantized and noise corrupted measurements of the output signal have been recently developed, also recursive least-squares (RLS) algorithm that using multiple time-varying for on-line parameter estimation of an induction machine (IM) was proposed and compared to other least square methods see [1, 2, 3, 4, 5, 6, 7, 8, 9].

Different control strategies and schemes were developed to control the electric machines, such as fuzzy logic, sensorless control scheme using an observer and pole placement techniques, sliding mode control, and pulse width modulation (PWM) control techniques see [10, 11, 12, 13, 14, 15, 16, 17]

Feedback-linearizing control strategies were presented, such as the current tracking controller and the torque controller, PID controller, and fractional-order controller, see [18, 19, 20].

Nonlinear control methods of electric machines such as feedforward/feedback control strategy, composite nonlinear feedback (CNF) control, and obtaining a compensator of a nonlinear input/output characteristic that reduced the tracking accuracy characteristic have been proposed in [21, 22, 23].

Other methods such as chopper method was used to control the terminal voltage such that the input DC voltage is chopped by Insulated Gate Bipolar Transistor(IGBT). Phase Locked Loop(PLL) offers a stable frequency controller system which was widely used in communications, instrumentation and motor controlled. A PLL system using Field Programmable Gate Array (FPGA)chip and an analog Voltage Controlled Oscillator (VCO) were synthesized. Phase comparator (phase detector) and programmable counter (frequency divider) were implemented in FPGA. The results showed that motor speeds were not affected under fluctuating loads, see [24].

As a first attempt of applying a new methodology to the important area of electric motors, we also recognize that there are potentially other methods that can be used in this application. We hope that this study will stimulate further studies in using different methods and comparing pros and cons in their practical aspects. In its structure, a quantizer is a static nonlinearity. As a result, the entire system is a Wiener system for which many algorithms were available [25, 26, 27, 28, 29]. Some traditional system identification methods of Wiener systems employ continuously invertible segments of the nonlinear functions to jointly identify the linear dynamic subsystem and the nonlinear static function. Quantized observations represent non-smooth and non-

invertible nonlinear functions. Such methods may need certain smoothing functions to accommodate such nonlinearity. For example, extended Kalman filters or standard adaptive observer design methods such as deadbeat design, pole placement, H^2/H^∞ filtering [30, 31, 32, 33], etc., often rely on local linearization, and hence may need some further extension.

Networked control systems have drawn increased attention recently [34, 35, 36] with impact of communication channels on stability and achievable performance as an important focus [37, 38, 39]. System identification and signal estimation under quantized observations have been explored in [40, 41, 42, 43]. Sampling and quantization collectively determine data flow rates, which were shown to be a critical factor in feedback stability and performance [35, 38]. These theoretical advancements, however, have never been applied and evaluated in motor control problems. One key component in this study is signal averaging filters that are essential part for system identification and signal estimation under quantized observations. Signal averaging has been used in many aspects of stochastic analysis [44, 45, 46]. Background materials on stochastic processes and related topics can be found in [47, 48, 49] and references therein.

1.3 Original Contributions

In this thesis several methodologies in real time and wireless control of Permanent Magnate Direct Current (PMDC) motors are introduced.

There are several original contributions in this research work.

1. Developing algorithms that can perform model estimation of PMDC motors parameters under binary-valued or quantized output measurements. While this methodology has been mathematically developed with some appealing convergence properties, it has never been applied to system identification of electric machines. Using binary or quantized sensors is challenging for system modeling, identification and control because they are nonlinear, discontinuous, and provide very limited information. The quantized sensors used in this work are more cost effective than other regular sensors.

2. Introducing threshold adaptation technique. Choosing thresholds is important for fast convergence in our algorithm and to achieve good estimation results. The main idea is that the best inverse sensitivity is achieved when accumulative distribution function F(.) has the largest slope. For Gaussian distributions, it is at 0 or when the probability value $\zeta = 0.5$. Consequently, one may tune the threshold towards $\zeta = 0.5$.

   In general, the threshold adaptation starts with a selection of the range $[\zeta_{low}, \zeta_{high}]$ of ζ in which the inverse sensitivity of the distribution function F is acceptable. When ζ is outside of this arrange, one adapts the threshold according to the

relative ζ value: If $\zeta < \zeta_{low}$, the threshold C is moved up so that ζ will increase in the next data block. Similarly for $\zeta > \zeta_{high}$. It should be pointed out that the threshold adaptation is to improve motor estimation accuracy when the targeted motor speed changes. If the set point does not change, threshold adaptation does not need to be implemented frequently.

3. Applying and developing optimal Quasi-Convex combination estimator (QCCE). It is obvious that each threshold C_i can generate an estimate of ω. A suitable combination of these estimates will lead to an asymptotically optimal estimator for θ (the identification parameters of the system) by achieving the Cramer-Rao lower bound. It should be noticed that combining thresholds and using optimal Quasi-Convex combination estimator will improve the identification accuracy. The results show the convergence of sample variance of the QCCE estimator to the theoretical CR lower bound.

4. Hardware implementation: In this part the parameter estimation method is evaluated experimentally. To implement the experimental platform, we utilize the following equipments and measurement devices that are connected into a testing platform.

    - The Renesas DC Motor Control Demonstration Kit (YMCRPR8C25).
    - The NI SCB-68 shielded I/O connector block for interfacing I/O signals to plug-in data acquisition (DAQ) devices with 68-pin connectors.
    - A desktop computer which has LabVIEW software installed (ver 2011).

- A digital multimeter.

5. Proposing wireless communication methods in motor control systems. This will add new dynamic subsystems into the feedback loop. Design variables for the communication systems such as sampling schemes and quantization levels, which are directly linked to their resource consumptions, interact with controllers to jointly affect feedback stability and performance and investigate the impact of communication strategies on motor feedback systems and derive some important guidelines in designing remotely controlled electric motors.

   Many automotive manufacturers are seeking wireless solutions for intra-vehicle control systems. More importantly, in networked systems such as unmanned aerial vehicles, mobile sensor teams, autonomous highway vehicle platoons, wireless communication channels become an integral part of the feedback loop. Introduction of communication channels mandates signal sampling, quantization, and estimation, and consequently adds new dynamic subsystems into the feedback loop.

6. Introducing remote control strategy that uses two communication channels. The first channel is from the motor speed measurement to the remote controller, and the second one is from the remote controller to the motor voltage input for the feedback control signal. These two channels may have different sampling periods and signal estimation schemes, leading to an asynchronous framework which is more flexible than the commonly-employed synchronous

sampling schemes. Our results will demonstrate that many components of design variables interact closely to determine feedback properties. These include sampling interval, quantization levels, signal estimation data windows, motor dynamics, controllers, and signal estimation algorithms.

CHAPTER 2: BACKGROUND

This chapter introduces some background and theory of the fundamental elements and supporting technologies used in this study. PMDC motors are essential parts of electric and hybrid vehicle powertrains and their auxiliary subsystems [50, 51, 52, 53]. In addition, PMDC motors have been extensively employed in diversified industrial applications such as battery powered devices, X-ray and tomographic systems [62, 65].

Due to variations in motor parameters, for efficient torque/speed control, thermal management, motor condition monitoring, and fault diagnosis of PMDC motors, it is essential that motor characteristics are captured in real-time operations.

2.1 PMDC Motors

2.1.1 Direct Current Motors

Electric machines are essential systems in electric vehicles and widely used in other applications. DC machines appeared in the 1800's when M. Faraday created a basic disc-type machine. Nowadays, DC motors are used in control systems, because the speed and torque can be easily controlled.

DC electric motor is a device which converts electrical energy into mechanical energy, which can be driven by direct current DC. The physical DC motor diagram consists of an armature which is the main part in DC motor that consists of coil made of copper wire wound on a core of soft iron. This coil should be in a rectangular shape

and insulated. A commutator which is used to reverse the direction of the armature current is an insulated ring that made from copper. A ring is fixed on each end of the coil. Both rings are connected with two small strips of carbon called brushes which are connected to a DC power supply. They rotate along with coil between the brushes . There are two main types of DC motors the brushed and brushless DC motors, which use internal and external commutation respectively to reverse the current in the windings in synchronism with rotation. The diagram of a physical DC motor is shown in Figure 1 [79]. A PMDC motor is similar to an ordinary DC Shunt motor except that the field of PMDC is provided by permanent magnets instead of salient pole wound field structure.

How does a PMDC motor work? In PMDC motor, a fixed magnetic field generated by the permanent magnets interacts with the perpendicular field induced by the currents in the rotor windings, thus creating a mechanical torque. As the rotor turns in response to this torque, the angle between the stator and rotor fields is reduced, so that the torque would be nullified within a rotation of 90 electrical degrees (an electrical degree is a unit of measurement for expressing the amount of rotation in electric machines). To sustain the torque acting on the rotor, permanent-magnet DC motors incorporate a commutator, fixed to the rotor shaft. The commutator switches the supply current to the stator so as to maintain a constant angle=90, between two fields. Because the current is continually switched between windings as the rotor turns, the current in each stator winding is actually alternating, at a frequency

proportional to the number of motor magnetic poles and the speed.

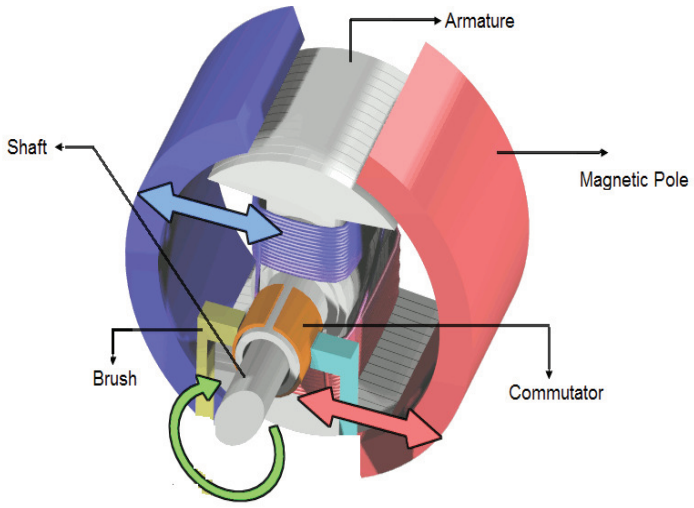

Figure 1: *Schematic Diagram of DC Motor*

There are five types of brushed DC motors:

1. Shunt DC motor: The rotor and stator windings are connected in parallel.

2. Separately excited motor: The rotor and stator are each connected from a different power supply, this gives another degree of freedom for controlling the motor over the shunt.

3. Series motor: the stator and rotor windings are connected in series. Thus the torque is proportional to the current so it gives the highest torque per current ratio over all other DC motors. It is therefore used in starter motors of cars and elevator motors.

4. Compound motor: the stator is connected to the rotor through a compound of shunt and series windings, if the shunt and series windings add up together, the motor is called cumulatively compounded. If they subtract from each other, then a differentially compounded motor results, which is unsuitable for any application.

5. Permanent magnet (PMDC) motors: The stator is a permanent magnet, so the motor is smaller in size. Figure 2 shows the types of brushed DC motor.

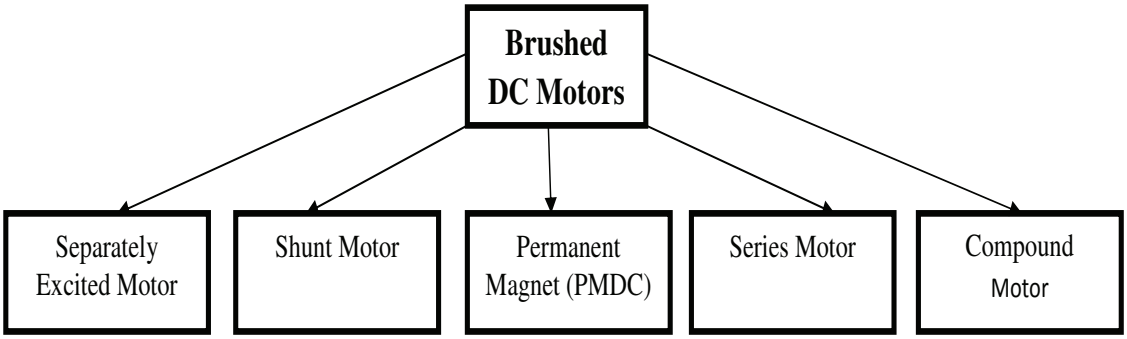

Figure 2: *Brushed DC Motor Types*

The second type is a brushless DC motor which is driven by controlled AC signals that use PWM or by direct DC supply. In brushless DC motors the commutator is replaced by external electronic switch synchronized to the rotor's position. Both brushed and brushless DC motors will be referred to simply as DC motors since both motor types can be represented by the same equations unless aspects of a specific type of motor are to be discussed [66, 67, 55].

2.1.2 Permanent Magnet Direct Current Motor (PMDC)

PMDC motors are dependent on permanent magnets to provide the magnetic field to produce torque, because PMDC motors do not have a field winding on the stator frame. This field is fixed, so it cannot be used for speed control. PMDC motors used high energy magnets made with neodymium or other strategic elements to minimize overall weight and size, most such are neodymium-iron-boron alloy .

PMDC motors have been extensively employed in industrial applications such as battery powered devices like wheelchairs and power tools, guided vehicles, welding equipment, X-ray and tomographic systems, CNC machines, etc. PMDC motors are physically smaller in overall size and lighter for a given power rating than induction motors. The unique features of PMDC motors, including their high torque production at lower speed, flexibility in design, make them preferred choice in automotive transmissions, gear systems, lower-power traction utility, and other fields [62, 54, 63, 64, 65].

For efficient torque/speed control, thermal management, motor condition monitoring, and fault diagnosis of PMDC motors, it is essential that their characteristics are captured in real-time operations. Although, PMDC motor models have been studied extensively and simplified electric/mechanical model structures have been widely used in system design and integration, during their operations component aging, drifting of their characteristics, faults, and interaction with operational environment make it highly desirable to estimate their model parameters in real time so that control

strategies can be adapted and faults can be promptly diagnosed [7, 60].

2.2 Speed Sensors

Speed sensors are used in rotating systems to achieve the information for both positional and frequency. They are widely used in vehicles, aerospace and monitoring machine applications. Using speed sensors the information of a time-varying voltage can be used to measure the speed as in tachometers.

Types of Speed Sensors:

1. Variable Reluctance Speed VR Sensors:

   It consists of four parts, a permanent magnet, a ferromagnetic pole piece, a pickup coil, and a rotating toothed wheel. Using this sensor the position and speed of moving metal components can be measured.

   The principal of work is depending on the gear teeth of the rotating wheel passing the face of the magnet, this will affect the amount of magnetic flux that flows through the magnet which leads to a change in coil reluctance. The flux is at a maximum when the gear tooth is closed to the sensor and the flux drops off when it is far away. The rotating of the wheel causes a time-varying flux, and then a proportional voltage in the coil is induced. After that a signal-processing circuitry is used to amplify the voltage across the coil and convert this to a speed according to mathematical relations.

   An advantage of this sensor is the low cost coil of wire and magnets. In addition

it can also be used in high-temperature applications, such as sensing the speed of a turbine of a jet engine or an engine cam shaft and crankshaft position control in an automobile. The disadvantage of this sensor is the complexity of circuit design to measure very-low-speed signals.

2. Eddy Current Speed Sensors:

   The relative motion of the field source and conductor results in electric currents induced in conductors, this causes changes in magnetic field with time. A circulating eddy current within the body of the conductor flows and thus induces magnetic fields. The faster the field changes are proportional to those circulating currents in the conductor.

3. RF Speed Sensors:

   RF speed sensors can be used to sense non-ferrous metals and nonmagnetic stainless steel like aluminum. It has large air gaps and sensing characteristics different from VR speed sensor. This sensor is not a passive device and requires coupling with a signal conditioners or preamplifier circuitry. The output of this sensor is pulses to measure the speed of moving object.

4. Hall Effect Sensors:

   A Hall Effect sensor is a transducer that varies its output voltage in response to a magnetic field. The applications of the Hall Effect sensor are proximity switching, positioning, speed detection, and current sensing. The disadvantages of this type of sensors in order to get high accuracy and performance are that

the Hall Effect sensors are more expensive. They also have limited maximum sensing distance and maximum operating temperature compared to other types. The functions of Hall effect sensor are shown in Figure 3.

Hall Effect sensors are widely used in measuring the speed of wheels and shafts, such as for tachometers, anti-lock braking, and internal combustion engine ignition timing systems. The Hall sensors can be also used in brushless DC electric motors to detect the position of the permanent magnet. Hall sensors are connected electronic signal conditioning circuit to get digital output. The Hall element is basically a small sheet of semiconductor material, if the biased Hall element is placed in a magnetic field, the output voltage is proportionally changed with respect to the strength of the magnetic field. The Hall Effect was discovered in 1879 by E. F. Hall.

A Hall Effect sensor is a binary-valued position sensor, whose output indicates only when the rotor magnet strips pass the position of the sensor installation. Each magnet strip defines a binary threshold on the rotor position [75, 76, 77, 78, 80, 81, 82].

2.3 System Identification and Parameter Estimation

In (Zadeh1962) the identification is determined on the basis of input and output, of a system within a class of systems, to which the system under test is equivalent. Parameter estimation is the experimental determination of values of the parameters

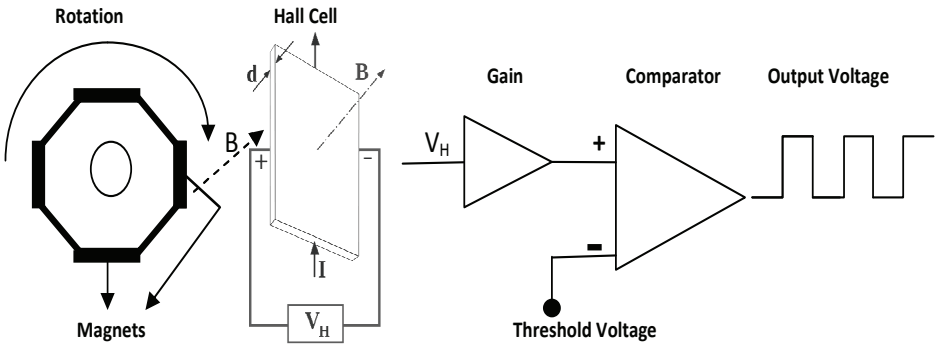

Figure 3: *Functions of a Hall Effect Sensor*

that govern the dynamic and/or non-linear behavior, assuming that the structure of the model is known.

Mathematical model is preferred in system identification. A mathematical model gives a description of the dynamic behavior of a system or process in either the time or frequency domain. Mathematical models have the ability to provide the foundation of most methods of engineering problems and design. In dynamic systems it is important to have the mathematical models for system identification and parameter estimation. These models can be formed using linear or nonlinear differential equations. The system identification is the most common approach which starts from measurements of the behavior of the system and the external influences (inputs to the system) and try to determine a mathematical relation between them without going into the details of what is actually happening inside the system. In this approach, the input is known and the output can be measured, so the unknown blackbox system can be identified from input and output. Two types of models are common in the field of system

identification:

Grey box Model: A certain model based on both insight into the system and experimental data is constructed. This model does however still have a number of unknown free parameters which can be estimated using system identification. Grey box modeling is also known as semi-physical modeling. Point out that the search for a good fit to experimental data tends to lead to an increasingly complex model.

Blackbox Model: In this model, there is no any prior model available for this type. Knowing that, most system identification algorithms are of this type.

In parameter estimation the input is known, the output can be measured, and the model is identified, so from the output and predicted output that achieved from the model we can estimate the parameters of the unknown blackbox system. After that model validation can be achieved by comparing the actual output with the estimated output [56, 57, 58, 59]. Figure 4 below shows the system identification and parameter estimation process.

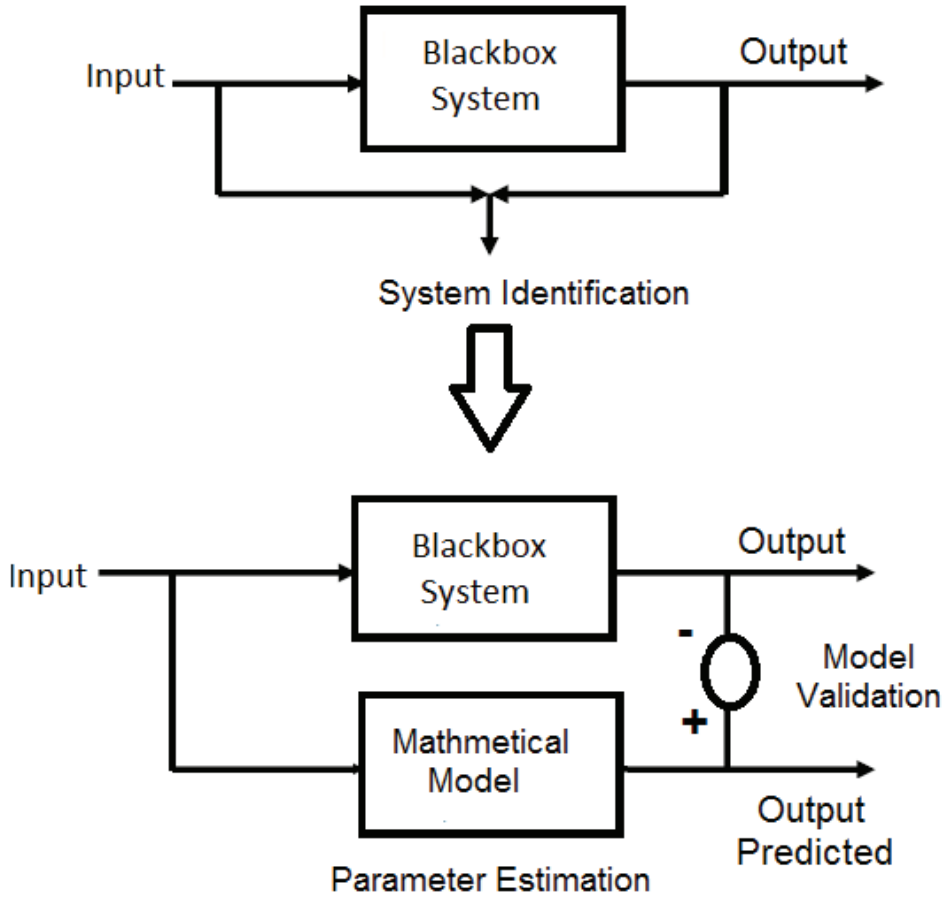

Figure 4: *System Identification and Parameter Estimation*

2.4 System Identification with Quantized Observations

The quantization measurements are inherent in the digital systems. This is simply because the data is received from a communication channel or using analog to digital converter. This idea can be expanded in the control systems networking process when the input and output signals are transmitted/received through a communication channel.

Equal-length intervals of the output range are the mostly common used in quantization. In this dissertation, a finite collection of subsets were used. The subsets may have equal or unequal lengths. In our study case, the subsets is fixed due to sensor limitations.

For the purpose of system identification the use of quantized measurements of inputs and outputs in the control systems is very important. It is proved that the identification error is reduced and the accuracy of the system increased using quantization data. It can be assumed, that the quantizer, in many situations is fixed and known, however this is not always the case. In automatic control, the quantizer may not be known, because it is adaptive.

Signal quantization and data compression are a typical analog to digital conversion process that has been studied extensively in the signal processing and computer science community. Studies of impact of quantization errors can be conducted in a worst-case or probabilistic framework, depending on how quantization errors are modeled.

Quantized sensors are used in dynamic systems since they are more cost effective than other regular sensors. They are preferable in real time applications. The quantizer is a fundamental block in the systems that used communication channels to transfer the data. Because quantization sensors have limited information this contains only a finite number of possible values, therefore, it is necessary to develop new methodologies and algorithms to achieve convergence of estimate methods [7, 8, 9, 83, 84].

Industry-grade sensors are quite expensive. It is important for cost reduction to use cheap sensors. For instance, to reduce packaging costs and enhance reliability, the number of magnet strips on the rotor needs to be reduced. The emerging field is using PMDC motors in remote controlled mode through communications, such as remote operated unmanned ground and aerial vehicles, mobile sensors, implanted medical devices. This has ushered in a new paradigm in which the system outputs must be communicated through a wireless network. In such applications, data flow rates are directly related to power consumption and bandwidth demands. Using measurement data of low length can dramatically reduce the consumption of communication resources. The main question is: Can one still achieve similar capability of real-time model estimation and control quality under the reduced complexity on the sensor system? This is a typical parameter estimation and signal recovery under quantized sensors.

Using binary or quantized sensors is challenging for system modeling, identification and control since they are nonlinear, discontinuous, and provide very limited

information. Typical nonlinear filtering techniques require smooth nonlinear functions or are of infinite dimensional (such as Wonham filters) [68, 69, 70]. The use of quantized sensors on modeling, identification, control, and diagnosis for electric machines is unique. This will have an impact on applications of electric machines in medical applications, vehicles with cheap sensors, and remote control with wireless communications.

2.5 Signal Estimation

In typical applications of control systems with communication channels, an output signal $y(t)$ is sampled to generate a sampled sequence $y_k = y(kT)$, quantized to produce quantized sequence $s_k = \mathcal{S}(y_k + d_k)$, where d_k is the measurement noise. Signal estimation aims to recover y_k from s_k.

To understand the fundamental aspect of this process, we consider the basic problem of binary-valued sensors of a threshold γ_k, which may be a constant γ or adapted for improved performance. In this case, the sensor output is $s_k = 1$, if $y_k + d_k \leq \gamma_k$, and $s_k = 0$, if $y_k + d_k > \gamma_k$.

The basic ideas are derived from system identification with binary-valued sensors [68, 93]. However, modifications must be made due to two fundamental differences here: (1) Signals are time varying; (2) Estimation cannot use progressively long-time windows for convergence. In this thesis, technical results on output estimation require some conditions on $y(t)$ so that y_k is slowly time varying.

2.5.1 Weighted Empirical Measures

For the same case $y_k = \theta$ and $\gamma_k = \gamma$, empirical measures was modified by the following truncated and exponentially weighted empirical measure. For a selected $0 < \alpha < 1$, define

$$\zeta_k^0 = (1 - \alpha) \sum_{l=0}^{\infty} \alpha^l s_{k-l} \tag{2.1}$$

where the weight is normalized to $(1-\alpha)\sum_{l=0}^{\infty}\alpha^l = 1$, and

$$\zeta_k = \begin{cases} \zeta_k^0, & \text{if } z \le \zeta_k^0 \le 1-z; \\ z, & \text{if } \zeta_k^0 < z; \\ 1-z, & \text{if } \zeta_k^0 > 1-z. \end{cases} \quad , \quad \widehat{y}_k = \gamma - F^{-1}(\zeta_k). \tag{2.2}$$

Remark 1 For practical applications, sequences start at certain starting time k_0. In that case (2.1) is modified to

$$\zeta_k^0 = \frac{1-\alpha}{1-\alpha^{k-k_0}} \sum_{l=0}^{k-k_0-1} \alpha^l s_{k-l}$$

to ensure that ζ_k^0 is unbiased, $E\zeta_k^0 = p$. To capture the "persistent" aspect of the signal estimation problem, we are considering the case when $k-k_0$ is large, eliminating the transient. This is achieved by letting $k_0 \to -\infty$, leading to (2.1).

Theorem 1

$$\lim_{\alpha\to 1} \frac{1+\alpha}{1-\alpha} E(\zeta_k - E\zeta_k)^2 = F(\gamma-\theta)(1-F(\gamma-\theta)) \tag{2.3}$$

$$\lim_{\alpha\to 1} \frac{1+\alpha}{1-\alpha} E(\widehat{y}_k - \theta)^2 = \frac{F(\gamma-\theta)(1-F(\gamma-\theta))}{f^2(\gamma-\theta)}. \tag{2.4}$$

Remark 2 Since $1+\alpha \to 2$ as $\alpha \to 1$, the claims of the theorem may also be written as

$$\lim_{\alpha\to 1} \frac{E(\zeta_k - E\zeta_k)^2}{1-\alpha} = \frac{F(\gamma-\theta)(1-F(\gamma-\theta))}{2}.$$

and

$$\lim_{\alpha\to 1} \frac{E(\widehat{y}_k - \theta)^2}{1-\alpha} = \frac{F(\gamma-\theta)(1-F(\gamma-\theta))}{2f^2(\gamma-\theta)}.$$

Proof: By the choice of z, $z < p < 1 - z$. Since $Es_{k-l} = p = F(\gamma - \theta)$, we have $E\zeta_k^0 = p$ and $E(\zeta_k^0 - p)^2 = \frac{1-\alpha}{1+\alpha}p(1-p)$. By the definition of ζ_k,

$$E(\zeta_k - \zeta_k^0)^2 = \int_0^z (x-z)^2 f_0(x)dx + \int_{1-z}^1 (x-z)^2 f_0(x)dx$$

where $f_0(x)$ is the density function of ζ_k^0. The first term is bounded by

$$\begin{aligned}\int_0^z (x-z)^2 f_0(x)dx &= \int_0^z (x-p+p-z)^2 f_0(x)dx \\ &\le \frac{1-\alpha}{1+\alpha}p(1-p) + (p-z)^2 P\{\zeta_k^0 \le z\} \\ &\le \frac{1-\alpha}{1+\alpha}p(1-p) + \frac{1-\alpha}{1+\alpha}p(1-p)\end{aligned}$$

by the Chebyshev inequality. Similar inequality can be derived for the second term.

As a result, we have

$$\lim_{\alpha \to 1} E(\zeta_k - \zeta_k^0)^2 = 0. \tag{2.5}$$

Hence, we can concentrate on ζ_k^0 in the following proof.

(1)

$$\begin{aligned}E(\zeta_k^0 - E\zeta_k^0)^2 &= (1-\alpha)^2 \sum_{l=0}^{\infty} \alpha^{2l} E(s_{k-l} - Es_{k-l})^2 \\ &= (1-\alpha)^2 \sum_{l=0}^{\infty} \alpha^{2l} p_{k-l}(1-p_{k-l}) \\ &= F(\gamma-\theta)(1-F(\gamma-\theta))\frac{1-\alpha}{(1+\alpha)},\end{aligned}$$

where we have used $p_k = P\{s_k = 1\} = F(\gamma - \theta)$.

(2) Since $p = Es_j = F(\gamma - \theta)$, we have $\theta = \gamma - F^{-1}(p)$ and $\widehat{y}_k - \theta = F^{-1}(\zeta_k) - F^{-1}(p)$. Furthermore, $E\zeta_k^0 = (1-\alpha)\sum_{l=0}^{\infty} \alpha^l Es_{k-l} = p$. Since $(1-\alpha)\sum_{l=0}^{\infty} \alpha^l = 1$, by Assumption 1,

$$\begin{aligned}E(\zeta_k^0 - p)^2 &= (1-\alpha)^2 \sum_{l=0}^{\infty}\sum_{m=0}^{\infty} \alpha^{l+m} E(s_{k-l} - p)(s_{k-m} - p) \\ &= \frac{1-\alpha}{1+\alpha}p(1-p) = \frac{1-\alpha}{1+\alpha}(F(\gamma-\theta)(1-F(\gamma-\theta)).\end{aligned}$$

Now, by a Taylor expression, there is a p_k^* such that

$$\begin{aligned}\widehat{y}_k - \theta &= F^{-1}(\zeta_k) - F^{-1}(p) \\ &= (F^{-1}(p))'(\zeta_k - p) + \frac{1}{2}(F^{-1}(p_k^*))''(\zeta_k - p)^2,\end{aligned}$$

where by $(F^{-1}(p))' = \dfrac{1}{f(\gamma-\theta)}$. Consequently,

$$\begin{aligned}&\frac{1+\alpha}{1-\alpha}|E(\widehat{y}_k - \theta)^2 - \frac{1}{f^2(\gamma-\theta)}E(\zeta_k^0 - p)^2| \\ &\leq \frac{1+\alpha}{1-\alpha}(\kappa_1|E(\zeta_k^0 - p)^3| + \kappa_2 E(\zeta_k - p)^4)\end{aligned} \tag{2.6}$$

for some constants κ_1 and κ_2. As higher order terms, we have

$$\frac{1+\alpha}{1-\alpha}(\kappa_1|E(\zeta_k^0 - p)^3| + \kappa_2 E(\zeta_k - p)^4) \to 0, \alpha \to 1.$$

Therefore,

$$\lim_{\alpha\to 1}\frac{1+\alpha}{1-\alpha}E(\widehat{y}_k - \theta)^2 = \lim_{\alpha\to 1}\frac{1+\alpha}{1-\alpha}\frac{1}{f^2(\gamma-\theta)}E(\zeta_k^0 - p)^2 = \frac{F(\gamma-\theta)(1-F(\gamma-\theta))}{f^2(\gamma-\theta)}.$$

□

2.5.2 Algorithms and Convergence

Let

$$v^* = \arg\min\ \sigma_{CR}^2(v) = \arg\min\frac{F(v)(1-F(v))}{f^2(v)}. \tag{2.7}$$

Since F and f are known, v^* can be calculated off-line and is a constant. The optimal threshold is related to v^* by $\gamma_k^* = v^* + y_k$. Consequently, when γ_k is adapted, the output estimation may be obtained as $\widehat{y}_k = \gamma_k - v^*$. Define $\mu = F(v^*)$.

Exponential averaging filters may be written recursively as

$$\widehat{y}_k = \widehat{y}_{k-1} + (1-\alpha)(x_k - \widehat{y}_{k-1}) \tag{2.8}$$

which is a stochastic approximation algorithm with a constant step size $\beta = 1 - \alpha$.

Weighted Empirical Measure Averaging with Threshold Adaptation

Consider the following algorithm

$$\begin{aligned} s_k &= \begin{cases} 1, & y_k + d_k \leq \gamma_k \\ 0, & y_k + d_k > \gamma_k \end{cases} \\ \xi_{k+1} &= \xi_k + \beta(s_{k+1} - \xi_k) \\ \gamma_{k+1} &= \gamma_k + \beta(\mu - \xi_k) \\ \widehat{y}_k &= \gamma_k - v^*. \end{aligned} \tag{2.9}$$

2.6 Control Theory

Linear Time Invariant (LTI) systems combine between two properties:linearity and time invariant system.

Linearity: a Linear system is the system that has a linear relationship between the input and the output :

If input u_1 produces output y_1 and input u_2 produces output $y_2$then,

$c_1u_1 + c_2u_2$ produces the output $c_1y_1 + c_2y_2$ where c_1 and c_2 are constants.

Time invariant system: the system is time invariant if the output does not depend on the time, in other words if we apply an input to the system now or after τ seconds from now, the output will be identical except for a time delay of the τ seconds.

That is, if the output due to input $u(t)$is $y(t)$, then the output due to input $u(t-\tau)$ is $y(t-\tau)$. Thus any system modeled as a linear homogeneous differential equation with constant coefficients is an LTI system.

Analyzing LTI systems are considered easy, compared to the time-varying and nonlinear systems.

Causality: A system is causal if the output depends only on present and past input, but not future. A necessary and sufficient condition for causality is

$\delta(t) = 0$ for all $t < 0$, where $\delta(t)$ is the impulse response.

Stability: A system is stable if for bounded-input the output is bounded, (i.e. for every bounded input, the output is finite).

$\| u(t) \|_\infty < \infty$ then the output is

$$\| y(t) \|_\infty < \infty$$

Discrete Time Systems:

The discrete time system has the following characterestics:

- Discrete-time models describe relationships between sampled variables $u(kT_s), y(kT_s), k = 0, 1, ...$
- During the sampling interval $[kT_s, (k+1)T_s)$, the value $u(kT_s)$is kept constant, where T_s is the sampling rate.
- A discrete-time signal can either represent the sampling of a continuous-time signal, or be an intrinsically discrete signal.
- Discrete-time signals are at the basis of digital controllers.

The types of control:

1. Feedback closed loop control: The output of the system $y(t)$ is fed back through a sensor measurement F to the reference value $r(t)$. The controller then takes the error (difference) between the reference and the output to change the inputs u to the system under control plant.
2. Open loop control: The controller doesn't know the output of the system.

The advantages and disadvantages of the two types of control systems.

Open Loop Systems:

Advantages:

- Simplicity and stability: they are simpler in their layout and hence are economical and stable due to their simplicity.
- Construction: Since these are having a simple layout so are easier to construct.

Disadvantages:

- Accuracy and Reliability: since these systems do not have a feedback mechanism, so they are very inaccurate in terms of result output and hence they are unreliable too.
- Due to the absence of a feedback mechanism, they are unable to remove the disturbances occurring from external sources.

Closed Loop Systems:

Advantages:

- Accuracy: They are more accurate than open loop system due to their complex construction. They are equally accurate and are not disturbed in the presence of non-linearities.

- Noise reduction ability: Since they are composed of a feedback mechanism, so they clear out the errors between input and output signals, and hence remain unaffected to the external noise sources.

Disadvantages:

- Construction: They are relatively more complex in construction and hence it adds up to the cost making it costlier than open loop system.
- Since it consists of feedback loop, it may create oscillatory response of the system and it also reduces the overall gain of the system.
- Stability: It is less stable than open loop system but this disadvantage can be stroked off since we can make the sensitivity of the system very small so as to make the system as stable as possible.

Transfer Function: A transfer function is used to describe the input and output relation of a system and hence serves as a model of the system. Such a transfer function model is most suitable for linear time-invariant systems with a single input and a single output. If the system to be controlled is nonlinear, or time-varying, or has multiple inputs or outputs, then it will be difficult, if not impossible, to model it by a transfer function.

The state variables of a system are defined as a minimum set of variables such that the knowledge of these variables at any time t_0, plus the information on the input subsequently applied, is sufficient to determine the state variables of the system at

any time $t > t_0$. If a system has n state variables, we say that the order of the system is n.

Hence the state space representation of LTI system can be written as

$$\dot{x} = Ax + Bu$$

$$y = Cx + Du$$

where A, B, C, D are matrices of appropriate dimensions. Since A, B, C, D are constants.

2.6.1 Digital PID Controller

In real systems, controllers are nowadays almost exclusively implemented digitally. Digital controllers are far more convenient to implement on microprocessors than are continuous-time controllers. Discrete-time controllers, are easily implemented using difference equations, i.e. simple computer software.

The PID controller becomes the most widely known and used one. There are many different types and design methods for the PID controller. Since many control systems using PID controller have proven satisfactory, it still has a wide range of applications in industrial control. PID controller popularity comes from its simplicity and its ability to be used in a wide variety of processes. PID controller has been an active research topic for many years.

The term PID stands for Proportional, Integral and Derivative. Each one of these letters (P, I, D) is term in a control algorithm, and each has a special purpose. It is possible to a PI controller, PD controller or P controller. It has been found from

the experimental point of view that the structure of the PID controller has sufficient flexibility to yield excellent results in many dynamic applications. Figure 5 shows the PID controller block diagram.

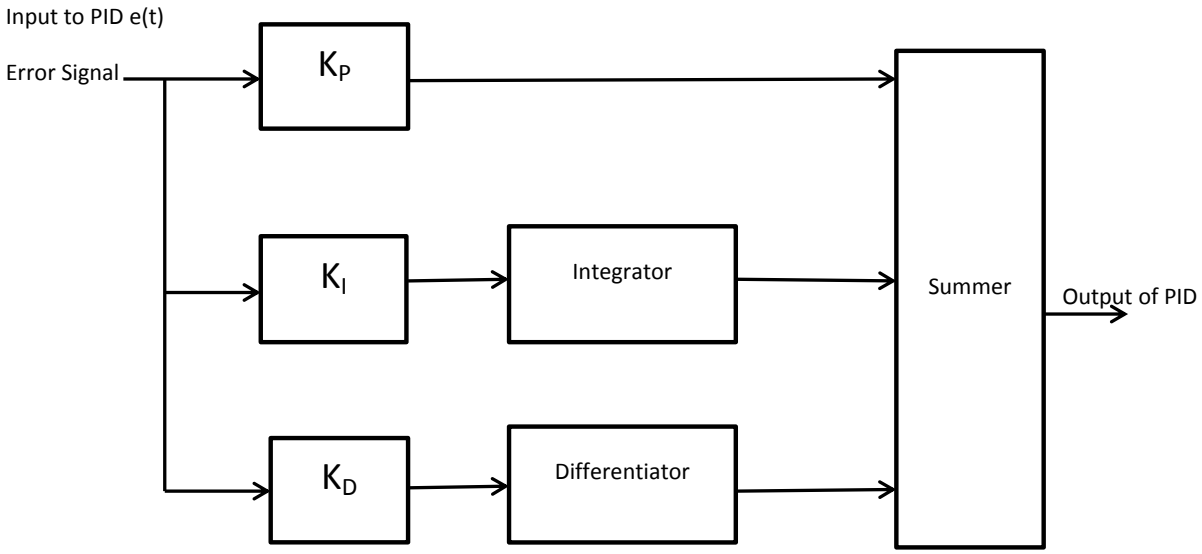

Figure 5: *PID Controller Block Diagram*

From the Figure 5, it can be clearly seen that in a PID controller, the error signal e(t) is used to generate the proportional, integral, and derivative actions, with the resulting signals weighted and summed to form the control signal $u(t)$ applied to the plant model.

A proportional controller K_P will have the effect of reducing the rise time and will reduce but never eliminate the steady-state error. An integral control K_I will have the effect of eliminating the steady state-error, but it may make the transient response worse. A derivative control K_D will have the effect of increasing the stability of the system, reducing the overshoot, and improving the transient response.

When designing a controller, the designer must define the specifications that need to be achieved by the controller. Normally, the maximum overshoot (Mp) of the system step response should be small. Commonly, a range between 2 percent and 10 percent is acceptable. Also the settling time t_s, is an important factor. The objective here is to design a PID controller so that the closed-loop [71, 72].

The relation between the Laplace transform variable s and the Z-transform variable z is $z = e^{sT}$, with sampling period T. We use a bilinear transformation (BLT) method from s-domain to z-domain, and then we have the following:

$e^{sT} \approx (1 + sT/2)/(1 - sT/2)$, Therefore define the BLT by

$z = (1 + sT/2)/(1 - sT/2)$ and its inverse is $s = 2/T(Z - 1)/(Z + 1)$

To convert a continuous transfer function $G(s)$ to a discrete transfer function $G(z)$ with sampling period T,then simply replaces all occurrences of s by

$2/T(Z - 1)/(Z + 1)$.

The continuous-time PID controller can be written in the form $C(s) = K_c[1 + 1/(\tau_I s) + \tau_D s]$

Where τ_I is the integration time constant or 'reset time', τ_D is the derivative time constant,

To convert this to digital form using the BLT, write

$C(z) = K_c[1 + 1/(\tau_I(2/T(z - 1)/(z + 1))) + \tau_D(2/T(z - 1)/(z + 1))]$

$= K_c[1 + (T(Z + 1))/(\tau_{ID}(z - 1)) + \tau_{DD}/T((z - 1)/(z + 1))]$

where the digital integral and derivative time constants are

$\tau_{ID} = 2\tau_I$, $\tau_{DD} = 2\tau_D$

More practical approach is to specify the closed loop transfer function so the realistic settling time is achieved.

If we have a scond order system represented as

plant: is

$$G(s) = K/((\tau_1 S + 1)(\tau_2 S + 1)), \text{ then the controller will be:}$$

$$C(s) = (\tau_1 + \tau_2)/(K\tau_c)[1 + 1/(\tau_1 + \tau_2)s + (\tau_1\tau_2)/(\tau_1 + \tau_2)s]$$

Comparing with

$$C(s) = K_c[1 + 1/(\tau_I s) + \tau_D S]$$

$$\text{Where } K_c = (\tau_1 + \tau_2)/(K\tau_c), \tau_I = (\tau_1 + \tau_2), \tau_D = (\tau_1\tau_2)/(\tau_1 + \tau_2)$$

To convert this to digital form using the BLT, then

$$C(z) = K_c[1 + (T(Z + 1))/(\tau_{ID}(z - 1)) + \tau_{DD}/T((z - 1)/(z + 1))]$$

2.6.2 Response Performance of Output Signal

There are four different types of input signals that can be used to measure the out performance response of the system:

- Impulse signal: In the time domain, $u(t) = c\delta(t)$. In the s domain, $U(s) = c$.
- Step signal: In the time domain, $u(t) = c$. In the s domain, $U(s) = \frac{c}{s}$.
- Ramp signal: In the time domain, $u(t) = ct$. In the s domain, $U(s) = \frac{c}{s^2}$.
- Sinusoidal signal: In the time domain, $u(t) = csin(2\pi ft)$. In the s domain, $U(s) = \frac{2\pi ftc}{s^2+(2\pi ft)^2}$.

where c is a constant in all the above.

In order to analyze system characteristics we can employ one of the input signals. If the inputs to a control system are gradually changing signals of time, then a ramp signal of time may be a good test signal. Similarly, if a system is subjected to sudden disturbances, a step signal of time may be a good test signal, and for a system subjected to a shock input, an impulse signal may be best. The time response of a control system consists of two parts:

1. Transient Response :The transient response is defined as the part of the time response which goes from the initial state to the final state and reduces to zero as time becomes very large.

2. Steady State Response. The steady-state response is defined as the behavior of the system as t approaches infinity after the transients have died out.

Thus the system response $y(t)$ may be written as: $y(t) = y_{tran}(t) + y_{ss}(t)$ where $y_{tran}(t)$ denotes the transient response, and $y_{ss}(t)$ denotes the steady-state response.

Some basic definitions for step response performance measure:

- Maximum overshoot: The maximum amount by which the system output response proceeds beyond the desired response. Let y_{max} denotes the maximum value of $y(t)$, and $y_{ss} = y(\infty)$ the steady-state value of $y(t)$, then the maximum overshoot of $y(t)$ is defined as: $M_P = y_{max} - y_{ss}$ The maximum overshoot is often represented by a percentage of the final value of the step response.

- Peak time, t_{max}: The time required for the response to reach the first peak of the overshoot.

- Rise time, t_r: The time required for the step response to rise from 10 to 90 percent of its final value.

- Settling time,t_s: The time required for the step response to settle within a certain percentage (2 or 5 percent) of its final value.

Figure 6 shows the step performance and how to measure the rising, settling, peak times and overshoot [71, 72].

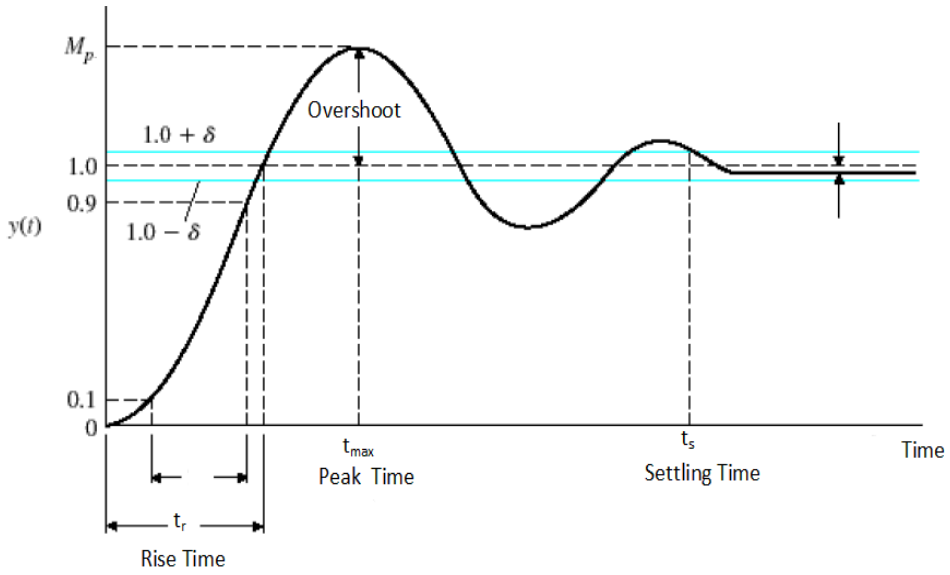

Figure 6: *Step Response with Performance Measure Times*

The transient behavior of a second-order system can be described by:

- The swiftness of the response, as represented by t_r and t_{max}

- The closeness of the response to the desired response, as represented by M_P and t_s.

CHAPTER 3: MODELS OF PMDC MOTORS

In this chapter I will derive and explain in details the models of PMDC motors. Three types of models will be introduced. First, the continuous- time models, secondly I will derived the discretized model , and finally a regression model will be discussed.

3.1 Continuous-Time PMDC Models

Typical models for DC motors contain one differential equation for the electric part, one differential equation for the mechanical part, and their interconnections. The state space model structure and derivations are quite standard. We summarize them below for self containment.

The equations for the motor rotor and shaft motion and stator wiring are

$$\frac{dw(t)}{dt} = \frac{-\mu}{J}\omega(t) + \frac{k_m}{J}i_a(t) - \frac{1}{J}T_L(t),$$

$$\frac{di_a(t)}{dt} = \frac{-k_b}{L_a}\omega(t) - \frac{R_a}{L_a}i_a(t) + \frac{1}{L_a}U(t),$$

which can be expressed in a state space model as

$$\dot{x}(t) = A_0x(t) + B_0u(t)$$

$$y(t) = C_0x(t)$$

where the state variables are $x(t) = [\omega(t), i_a(t)]'$, the inputs $u(t) = [T_L(t), U(t)]'$ and $A_0 = \begin{bmatrix} -\mu/J & k_m/J \\ -k_b/L_a & -R_a/L_a \end{bmatrix}$, $B_0 = \begin{bmatrix} -1/J & 0 \\ 0 & 1/L_a \end{bmatrix}$, $C_0 = \begin{bmatrix} 1 & 0 \\ 0 & 1 \end{bmatrix}$.
where,

$\omega(t)$ is the shaft speed (rad/sec),

$i_a(t)$ the motor current (A),

$U(t)$ the supply voltage (V),

$T_L(t)$ the load torque (N.m),

J the moment of inertia for the motor (Kg.m^2),

μ the friction coefficient (N.m.s),

k_m the motor constant (N.m/A),

k_b the back emf constant (V/rad/s),

L_a the armature inductance (H),

and R_a the armature resistance (Ohm).

The transfer matrix of the system can be derived as

$$G(s) = \frac{1}{(s+\frac{\mu}{J})(s+\frac{R_a}{L_a}) + \frac{k_m k_b}{L_a J}} \begin{bmatrix} -\frac{s+\frac{R_a}{L_a}}{J} & \frac{k_m}{L_a J} \\ \frac{k_b}{L_a J} & \frac{s+\frac{\mu}{J}}{L_a} \end{bmatrix}.$$

From the above expressions, we obtain the shaft rotational speed and armature current as functions of the input voltage and load disturbance

$$\Omega(s) = \frac{-(L_a s + R_a)T_L(s) + k_m U(s)}{(Js+\mu)(L_a s + R_a) + k_m k_b},$$

$$I_a(s) = \frac{(Js+\mu)U(s) + k_b T_L(s)}{(Js+\mu)(L_a s + R_a) + k_m k_b}.$$

In particular, the transfer function from the input voltage $U(s)$ to the angular speed

$\Omega(s)$ is

$$G_1(s) = \frac{k_m/L_aJ}{s^2 + \left(\frac{R_a}{L_a} + \frac{\mu}{J}\right)s + \frac{R_a\mu + k_mk_b}{L_aJ}}.$$

Denote $r = \frac{R_a}{L_a} + \frac{\mu}{J}$, $d = \frac{R_a\mu + k_mk_b}{L_aJ}$, $g = \frac{k_m}{L_aJ}$.

It follows that

$G_1(s) = \frac{g}{s^2+rs+d} = \frac{g}{(s-s_1)(s-s_2)}$

where $s_1 = (-r + \sqrt{r^2 - 4d})/2$, $s_2 = (-r - \sqrt{r^2 - 4d})/2$ are the poles of $G_1(s)$.

3.2 Discretization of PMDC Models

For system identification, it is convenient to use a discretized model in a regression structure. Suppose that the sampling interval is T (second). Denote the sampled signals

$$\omega_k = \omega(kT), u_k = U(kT), k = 0, 1, \ldots$$

Using the partial fraction expansion and zero-order hold function, the corresponding discrete-time transfer function of the sampled system can be derived via the standard z-transform as $\frac{\widetilde{\Omega}(z)}{\widetilde{U}(z)} = \left(\frac{G_1(s)\left(1-e^{-Ts}\right)}{s}\right) := \widetilde{G}_1(z)$ Here, $\widetilde{\Omega}(z)$ and $\widetilde{U}(z)$ are the z-transforms of the speed and voltage sampled sequences, respectively.

Under a step input with amplitude M, the angular speed is $\widetilde{\Omega}(z) = \widetilde{G}_1(z)\left(\frac{M}{1-z^{-1}}\right)$. This implies that

$$\omega_k = M(c_1 + c_2e^{s_1kT} + c_3e^{s_2kT}), \tag{3.10}$$

where $c_1 = \frac{p}{s_1s_2}$, $c_2 = \frac{p}{(s_1(s_1-s_2))}$, $c_3 = \frac{p}{(s_2(s_2-s_1))}$. Accuracy of the discretized models is demonstrated in the following case study.

Example 1 Suppose that the above system is simulated over the time interval $[0, 2]$ second with the sampling period $T = 0.01$ sec. The input voltage is a step function with amplitude $M = 240$ V. The motor specification values as supplied by the manufacturer are as follows: $L_a = 0.0104$ H, $R_a = 1.43$ ohm, $J = 0.068\ Kg.m^2$, $\mu = 0.0415\ N.m.s$, $k_m = k_b = 1.8\ N.m/A$ or $V/rad/s$. Figure 7 shows the open-loop speed trajectories of the PMDC motor in continuous and discrete forms. The discretized models are sufficiently accurate for system identification and control.

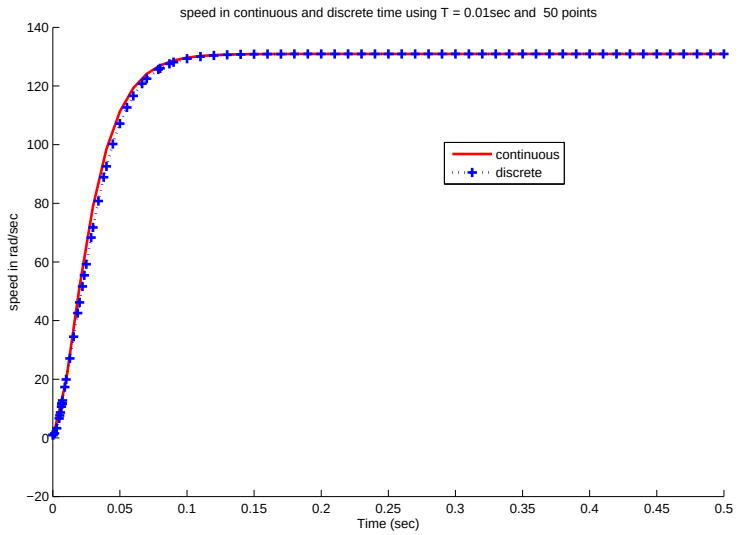

Figure 7: *Continuous-time and discrete-time speed of the PMDC motor*

3.3 Regression Models

For system identification experiments, it is desirable to transform a model into a regression form. The general form for the speed can be written in an autoregressive moving average with input (ARMA or ARMAX)[1] model [7, 61, 60] as

$$\omega_k = \sum_{j=1}^{n} a_j \omega_{k-j} + \sum_{i=0}^{n} b_i u_{k-i},$$

where n is the model order. In our case, the PMDC motor is assumed to have the following ARMA model ($n = 2$) structure

$$\omega_k = [\omega_{k-1}, \omega_{k-2}, u_{k-1}, u_{k-2}] \begin{bmatrix} a_1 \\ a_2 \\ b_1 \\ b_2 \end{bmatrix} \tag{3.11}$$

where ω_k is the speed of PMDC motor (rad/sec) and u_k the input voltage of PMDC motor (V). It is a standard but tedious process to verify that the parameters are related to the original system parameters and the sampling interval by

$a_1 = -(e^{s_1 T} + e^{s_2 T})$,

$a_2 = e^{(s_1+s_2)T}$,

$b_1 = -(c_1 + c_2)e^{s_2 T} + c_2 + c_3 + (c_1 + c_3)e^{s_1 T}$,

$b_2 = c_2 e^{s_2 T} + c_1 e^{(s_1+s_2)T} + c_3 e^{s_1 T}$.

[1] To simplify notation, we will use ARMA to represent both ARMA and ARMAX models in this dissertation.

Now we can write the noise-free speed in an operator form as

$$\omega_k = \widetilde{G}(q)u_k = \frac{b_1 q + b_2 q^2}{1 - (a_1 q + a_2 q^2)} u_k, \quad k = 0, 1, 2, \ldots$$

where q is the one-step shift operator $qu_k = u_{k-1}$, or in the regression form

$$\omega_k = \phi_k^T \theta, \quad k = 0, 1, 2, \ldots$$

where $\phi_k^T = [\omega_{k-1}, \omega_{k-2}, u_{k-1}, u_{k-2}]$, $\theta = [a_1, a_2, b_1, b_2]$. The parameter vector θ is to be identified. When a random noise or dither d_k is added to the output ω_k, we have

$$y_k = \omega_k + d_k.$$

Remark 3 We use an ARMA model structure for system identification. For convenience of algorithm implementation, ARMA models have a few advantages: (1) Practical linearized systems have rational transfer functions. If they are represented by FIR (finite impulse response) models, finite truncation must be used, leading to unmodeled dynamics. To reduce truncation errors, the order of the FIR model must be relatively high. ARMA models do not introduce such errors and retain the same order as the original continuous-time system after sampling. (2) State space model realizations of a system are not unique and in general contain more parameters than their transfer functions. For this reason, most identification algorithms are based on input/output models. It is also noted that, the ARMA model structures are the basis for Box-Jenkins polynomial models in statistical time series analysis. Also, we are using the output error model (instead of equation error models) in representing the additive noises/dithers. This is used on the basis of the PM motor data measurement schemes.

CHAPTER 4: PARAMETER ESTIMATION OF PMDC MOTORS USING QUANTIZED SENSORS

Although motor dynamics involve nonlinearity due to distortion in magnetic fields, it is a standard practice that locally linearized models around operating points are used. In this case, the model parameters will change under different operating conditions. Operational environments such as temperature, humidity, wiring insulation, motor aging, etc., will result in further parameter deviations. This dissertation employs identification methods to capture such changes in real time. Consequently, linearized models with unknown parameters are suitable in this pursuit. In this study, we employ the typical linear state space models of PMDC motors [62, 65, 50]. The relationship between the input voltage and output speed of the motor can be derived and represented by a higher-order differential equation. Under a selected sampling interval, the system can be discretized to a regression model structure, which is suitable for system identification experiments. Depending on applications, position or speed control problems are typical. This dissertation is focused on speed control problems.

The motor rotational speed is measured by either a binary sensor or quantized observations. One key idea to make a binary sensor to provide as much information as a regular sensor is to add a small periodic dither to the voltage input. Due to inherent motor inertia, this small dither will not affect motor operations. However, this will greatly enhance the system identification capability. Under this dithered input, model parameters in a regression model structure can be individually identified,

substantially reducing algorithm complexity. Identification algorithms are developed and their convergence properties are established. It can be shown that by choosing the periodic dither properly, the regression matrix will become full rank. Consequently the input becomes "persistently exciting" for quantized identification, namely the input will be rich enough so that the model parameters can be identified from input and quantized output observations. The theoretical foundation of this technology was developed in [68, 69, 70]. This dissertation applies it into algorithms for PMDC motors and demonstrated its utility and capability in this important application area.

In this chapter, I will introduce the methodology of my work. Then, I will explain the binary identification method using single threshold. Finally, I will propose the quantization speed identification method using multi-thresholds.

4.1 Problem Formulation on Quantized Identification of PMDC Motor Parameters

If the output of the system is measured by a quantized sensor with m thresholds $-\infty < C_1 < \cdots < C_m < \infty$, the sensor output can be represented by a set of m indicator functions $s_k = [s_k(1), \ldots, s_k(m)]^T$, where $s_k(i) = I_{\{-\infty < y_k < C_i\}}, i = \{1, \ldots, m\}$. Here, for a generic set Q of real numbers, the indicator function is defined as

$$I_{\{y_k \in Q\}} = \begin{cases} 1, \text{ if } y_k \in Q \\ 0, \text{ otherwise} \end{cases}$$

This leads to a system configuration shown in Figure 8.

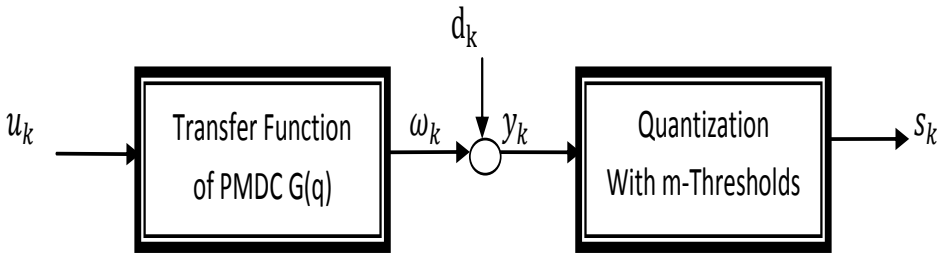

Figure 8: *Quantized system identification configuration*

We should point out that the "sensor" may be a physical sensor such as a Hall-effect sensor or it may represent a quantization/coding scheme if the output must be transmitted through a communication network.

In such a setting, the sensor may be viewed as m binary-valued sensors with increasing thresholds. Also, in their indicator function representation, if $s_k(i) = 1$, then $s_k(j) = 1$ for $j \geq i$. An alternative representation of the sensor is by $\tilde{s}_k(i) = I_{C_{i-1} < y_k \leq C_i}$ with $C_o = -\infty$, and $C_{m+1} = \infty$ with the interval (C_m, ∞). This representation employs distinct switching intervals. Consequently, only one $\widetilde{s}_k(i) = 1$ at any k.

Assumption 1 *Suppose that $\{d_k\}$ is a sequence of i.i.d. (independent and identically distributed) random variables. The accumulative distribution function $F(\cdot)$ of d_1 is a twice continuously differentiable function. The moment generating function of d_1 exists. The inverse of the function $F(\cdot)$ exists and is $F^{-1}(\cdot)$.*

4.2 Binary Identification of PMDC Motors

First, we consider the special case of binary sensors. The algorithms described in this section will then be generalized to quantized identification algorithms in the next section.

4.2.1 Observation Structures

Suppose that the output of the system is measured by a binary sensor with threshold C. The output of the sensor will be either 0 or 1 according to the following relation by an indicator function

$$s_k = I_{\{y_k \leq C\}} = \begin{cases} 1, y_k \leq C \\ 0, y_k > C \end{cases}.$$

Since the sensor output provides only the information whether the system output is above or below C, it contains very little information for the signal itself and is insufficient for system identification. However, if the system output is either corrupted by noise or is added with a stochastic dither, the statistical analysis can lead to much richer information on the system. Mathematically, by using the noise distribution information and the laws of large numbers in statistics, more accurate information of the system output can be asymptotically obtained from the $\{0, 1\}$ sequences of the sensor output.

In this framework, suppose that the output of the system has an additive noise/dither

d_k and the sensor output becomes

$$s_k = \mathcal{S}(\omega_k + d_k) = \begin{cases} 1, \omega_k + d_k \leq C \\ 0, \omega_k + d_k > C \end{cases}.$$

4.2.2 Identification Algorithms

The identification algorithms of this dissertation utilize periodic input signals, which are designed to simplify identification problems, provide persistent excitation, and make it possible to use the laws of large numbers directly in achieving parameter convergence. In this framework, the parameter vector θ of the transfer function $G(q)$ is to be estimated by using a binary sensor. The main algorithm is described below.

Select u_k to be a 4-periodic signal which is full rank, see [70] for detailed definitions and discussions of full rankness. Then the noise-free system output $\omega_k = G(q)u_k$ is also 4-periodic, after a short transient duration since the system is exponentially stable. Denote the first 4 values of the 4-periodic output sequence by ω_1, ω_2, ω_3, ω_4. Then other values of ω_k are $\omega_{1+4l} = \omega_1$, $\omega_{2+4l} = \omega_2$, $\omega_{3+4l} = \omega_3$, $\omega_{4+4l} = \omega_4$, for $l = 1, 2, \ldots$. Let $v_k(j) = \omega_j + d_k$ be the noise-corrupted output, $j = 1, 2, 3, 4$.

We take N samples on the sensor output. For convenience of notation, assume that N is a multiple of the size of θ, which is 4. Hence, let the observation length $N = 4L$ for some positive integer L. It follows that $s_{j+4l} = \mathcal{S}(\omega_j + d_{j+4l}), l = 0, 1, \ldots, L-1$. The basic idea is that we first obtain estimates $\widehat{\omega}_1$, $\widehat{\omega}_2$, $\widehat{\omega}_3$, $\widehat{\omega}_4$. Then the system parameter vector θ can be estimated from the model structure $\omega_k = G(q)u_k$.

Generically, suppose that ω_j, $j = 1, 2, 3, 4$, is an unknown speed. Then for any l,

the probability of the event $\{s_{j+4l} = 1\}$ is

$$p_j = P\{-\infty < v_{j+4l} \leq C\} = F(C - \omega_j). \tag{4.12}$$

Our approach is based on the fact that the probability p_j can provide more information about the unknown speed ω_j since the accumulative distribution function $F(\cdot)$ is known and invertible. This implies that

$$\omega_j = C - F^{-1}(p_j). \tag{4.13}$$

In other words, if one can estimate p_j, then (4.13) can be used to estimate ω_j. This leads to the following estimation algorithm.

Estimation Algorithms:

- Step 1: Estimation of p_j in (4.12).

  Take N measurements on s_k. Then for $j = 1, 2, 3, 4$,

  $$\zeta_L^j = \frac{1}{L} \sum_{l=0}^{L-1} s_{j+4l}$$

  is the sample relative frequency of v_{j+4l} taking values in $(-\infty, C)$.

- Step 2: Estimation of ω_j, $j = 1, 2, 3, 4$.

  An estimate $\widehat{\omega}_j$ of ω_j can be derived from

  $$\widehat{\omega}_j = C - F^{-1}(\zeta_L^j).$$

- Step 3: Construction of Periodic Estimates.

From the one-period estimated values $\widehat{\omega}_j, j = 1, \ldots, 4$, a 4-periodic extension can be constructed by $\widehat{\omega}_{j+4l} = \widehat{\omega}_j$ for $l = 0, 1, \ldots, L-1$. Then, for a given $j \in \{1, \ldots, 4\}$, the true output speed is related to the estimates by $\omega_{j+4l} = \widehat{\omega}_{j+4l} + \varepsilon_{j+4l}$, $l = 0, 1, \ldots, L-1$, where ε_{j+4l} is the estimation error.

- Step 4: To estimate the parameter θ, we use $\widehat{\omega}_k$ in place of ω_k, $\widehat{\omega}_k = \widehat{\phi}_k^T\theta + \varepsilon_k$, where

$$\widehat{\phi}_k^T = [\widehat{\omega}_{k-1}, \widehat{\omega}_{k-2}, u_{k-1}, u_{k-2}].$$

Denote

$$\widehat{\Omega} = \begin{bmatrix} \widehat{\omega}_3 \\ \vdots \\ \widehat{\omega}_{L-1} \end{bmatrix}, \widehat{\Phi} = \begin{bmatrix} \widehat{\phi}_3^T \\ \vdots \\ \widehat{\phi}_{L-1}^T \end{bmatrix}, E = \begin{bmatrix} \varepsilon_3 \\ \vdots \\ \varepsilon_{L-1} \end{bmatrix}.$$

Then, we have

$$\widehat{\Omega} = \widehat{\Phi}\theta + E. \tag{4.14}$$

- Step 6: Since the regression matrix $\widehat{\Phi}$ is full rank, one derives an estimate θ from $\widehat{\theta}_L = (\widehat{\Phi}^T\widehat{\Phi})^{-1}\widehat{\Phi}^T\widehat{\Omega}$.

4.2.3 Convergence Analysis

The theoretical foundation of the above algorithm follows [68, 69, 70], especially Theorem 3 in [69], with a specification on the model order $n = 2$ and data length L.

Theorem 2 *Suppose that $G(q) = \frac{D(q)}{B(q)}$, $D(q)$ and $B(q)$ are coprime polynomials, i.e., they do not have common roots. If $\{u_k\}$ is $2n$-periodic and full rank, then $\widehat{\theta}_L \to \theta$, w.p.1, as $L \to \infty$.*

Proof: Here, we only outline the main ideas of the proof. The details can be found in [69].

From $\widehat{\omega}_{j+4l} = \omega_{j+4l} + e_L^j$, (4.14) can be expressed as

$$\Omega + E_L = (\Phi + \varsigma(E_L))\widehat{\theta}_L, \tag{4.15}$$

where both E_L and $\varsigma(E_L)$ are perturbation terms with $E_L \to 0$ w.p.1 as $L \to \infty$, and $\varsigma(\cdot)$ is a continuous function of its argument satisfying $\varsigma(E_L) \to 0$ as $E_L \to 0$.

Since Φ has a uniformly bounded inverse and $\varsigma(E_L) \to 0$, w.p.1, $\Phi + \varsigma(E_L)$ is invertible w.p.1 for sufficiently large L. It follows that for sufficiently large L, by (4.15)

$$\Phi^T\Omega + \Phi^T E_L = (\Phi^T\Phi + \Phi^T\varsigma(E_L))\widehat{\theta}_L.$$

This implies that

$$\begin{aligned}\widehat{\theta}_L &= (\Phi^T\Phi + \Phi^T\varsigma(E_L))^{-1}(\Phi^T\Omega + \Phi^T E_L) \\ &\to (\Phi^T\Phi)^{-1}\Phi^T\Omega = \theta\end{aligned}$$

w.p.1 as $L \to \infty$. □

4.2.4 Examples

This section presents several examples. The main objective is to verify that the proposed parameter estimation methodology works properly. The PMDC motor model and the simulation results are performed by using the Matlab/Simulink software. The identification algorithm is applied to the system and the model parameter estimates

are derived. Estimation errors are evaluated by the total square error (TSE),

$$TSE = (\widehat{\theta}_L - \theta)^T (\widehat{\theta}_L - \theta).$$

Example 2 In this example, we apply a 4-periodic input voltage to the PMDC motor model in Example 1 with its first 4 values as $u_k = 240 \times [1, 0.9, 1.1, 0.85]$ V.

The binary sensor threshold is $C = 125$. The measurement noises are i.i.d. Gaussian noise sequences with zero mean and standard deviation $\sigma = 4$. The results are shown in Table 1. Figure 9 shows the speed trajectories for estimated and actual parameters.

Table 1: Parameter Estimation with $M = 240$ V, $\sigma = 4$, and $C = 125$

Para.	Actual	Est. N=1000	Est. N=5000	Est. N=10000	Est. N=20000
a_1	-1.0078	-0.8628	-0.9004	-1.0246	-1.0079
a_2	0.2513	0.2848	0.3123	0.2866	0.2723
b_1	0.0815	0.09378	0.07201	0.0882	0.0872
b_2	0.0514	0.0346	0.0421	0.0547	0.0571
TSE	-	0.02258	0.01543	0.00158	0.00051

Example 3 We consider the same system as in Example 2, with the observation length $N = 20000$, and the threshold value $C = 125$, but different noise standard deviation values σ. The results are shown in Table 2.

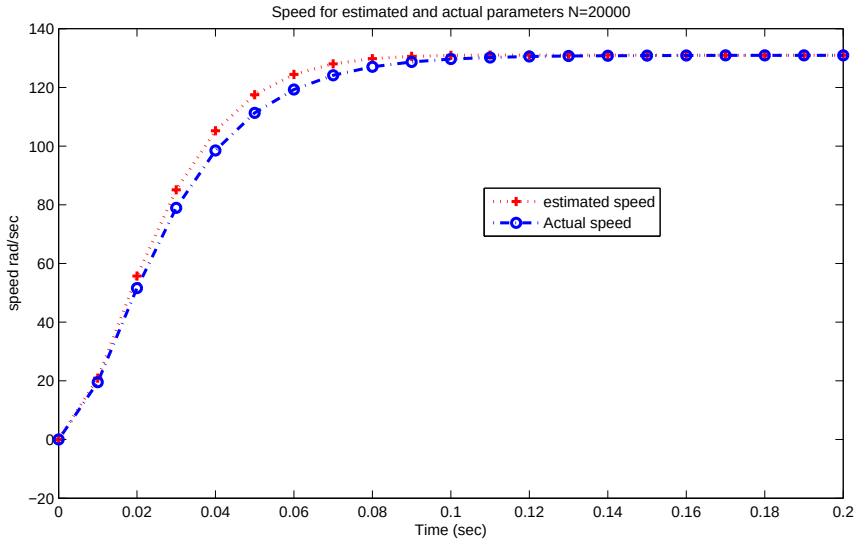

Figure 9: *The motor speed trajectories using actual and estimated parameters*

Table 2: Parameter Estimation $M = 240$ V, $N = 20000$, and $C = 125$

Para.	Actual	Est. $\sigma = 8$	Est. $\sigma = 12$	Est. $\sigma = 16$	Est. $\sigma = 25$
a_1	-1.0078	-1.0109	-1.0341	-0.8905	-0.8357
a_2	0.2513	0.2251	0.2972	0.3715	0.3276
b_1	0.0815	0.0648	0.1015	0.0621	0.0589
b_2	0.0514	0.0520	0.0423	0.03627	0.06381
TSE	-	0.00098	0.00328	0.02881	0.03610

Discussions:

- From Table 1 and Figure 9, we can see that the parameter estimation errors decrease as the observation length N increases, which is detailed by the total square errors. This is consistent with the laws of large numbers which claim that the convergence rates are proportional to $1/N$. Such a rate of convergence for binary sensors was derived in [69].

- It is noted from Table 2 that the standard deviation σ of the Gaussian noise shouldn't be too high, because this may affect the parameter estimation. But if the noise spread (defined by its standard deviation) changes, the estimation can be less accurate. The explanation for this situation is that when the inverse of the noise distribution function, which is used in the identification algorithm, becomes very big, estimation accuracy decreases. This observation indicates that the input design, threshold selection, and noise characterizations are closely related in ensuring identification accuracy. When they are properly selected, accuracy of parameter estimation can be substantially enhanced. In other words, with only a minor loss of convergence speed, we may use much cheaper sensors or much lower communication resources without much detrimental impact on modeling and control performance.

4.2.5 Threshold Adaptation

Choosing thresholds is important for fast convergence in our algorithm. Example 2 achieves good estimation results by using the threshold $C = 125$ which is close to the actual motor speed. To understand this, we use the following example in which different thresholds are used.

Example 4 We consider the same system as in Example 2, with a fixed noise standard deviation $\sigma = 4$, and the observation length $N = 20000$, but with different input amplitudes and different sensor threshold values. The results are shown in Table 3.

Table 3: Parameter Estimation with $N = 20000$ and $\sigma = 4$

Para.	Actual	Estimate u = 200 C = 105	Estimate u = 150 C = 79	Estimate u = 100 C = 55	Estimate u = 24 C = 12
a_1	-1.0078	-1.0102	-1.0072	-1.0223	-0.9497
a_2	0.2513	0.2584	0.2377	0.2819	0.2458
b_1	0.0815	0.0843	0.0762	0.085	0.1115
b_2	0.0514	0.0512	0.0496	0.0567	0.0500
TSE	-	6.4E-05	0.00022	0.00119	0.00431

Table 3 clarifies that the threshold value C has significant impact on identification accuracy. The thresholds should be chosen such that the values of ζ are near the range in which $F(\cdot)$ is invertible. Since the speed ω_k changes with time, the thresholds should be adapted. The threshold adaptation algorithm is outlined by the flowchart in Figure 10. The main idea is that the best inverse sensitivity is achieved when $F(\cdot)$ has the largest slope. For Gaussian distributions, it is at 0 or when $\zeta = 0.5$.

Consequently, one may tune the threshold towards $\zeta = 0.5$.

In general, the threshold adaptation starts with a selection of the range $[\zeta_{low}, \zeta_{high}]$ of ζ in which the inverse sensitivity of the distribution function F is acceptable. When ζ is outside of this arrange, one adapts the threshold according to the relative ζ value: If $\zeta < \zeta_{low}$, the threshold C is moved up so that ζ will increase in the next data block. Similarly for $\zeta > \zeta_{high}$. It should be pointed out that the threshold adaptation is to improve motor estimation accuracy when the targeted motor speed changes. If the set point does not change, threshold adaptation does not need to be implemented frequently.

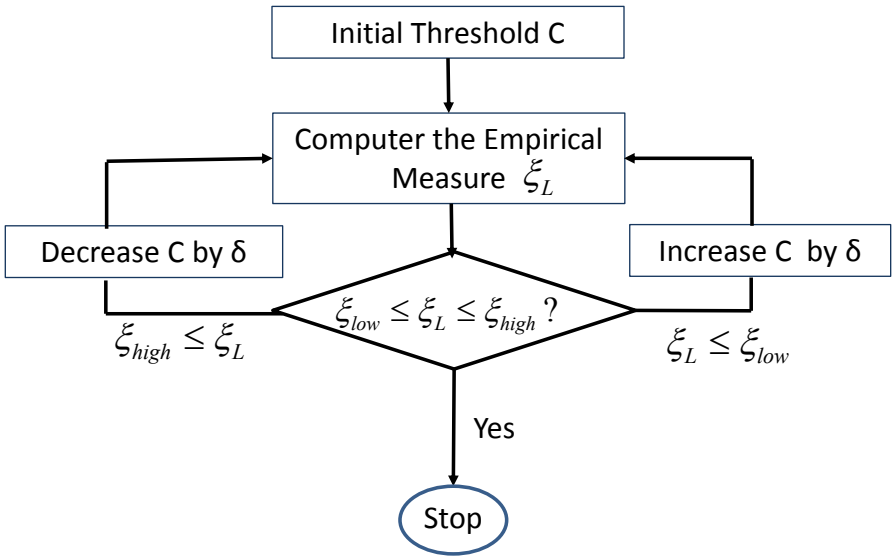

Figure 10: *Threshold adaptation flowchart*

4.3 Quantized Identification Algorithms

When more complicated quantized sensors are used, more information can be extracted from the sensor output which can potentially improve estimation accuracy. However, proper usage of the sensor information is far from a trivial issue. We will use a scheme that is optimal in the sense that the estimation error variance is minimized.

Suppose that now we have a quantized sensor with m thresholds $-\infty < C_1 < \cdots < C_m < \infty$, and the sensor output can be represented by a set of m indicator functions $s_k = [s_k(1), \ldots, s_k(m)]^T$, where $s_k(i) = I_{-\infty<y_k<C_i}, i = \{1, \ldots, m\}$. First, we observe that each threshold C_i is a binary sensor and $s_k(i)$ is the corresponding sensor output. Consequently, all discussions in the previous section on binary sensors are valid, including input design, algorithms, convergence properties, and impact of threshold selections. Since these binary sensors provide information on the same ω_j, $j = 1, 2, 3, 4$, the main issue here is how to combine information from these binary sensors of different thresholds to form a new combined estimate of the same quantity.

4.3.1 Optimal Quasi-Convex Combination Estimator

It is obvious that each threshold C_i can generate an estimate of ω. A suitable combination of these estimates will lead to an asymptotically optimal estimator for θ by achieving the Cramer-Rao lower bound.

Define the weighting $\gamma = [\gamma_1, \ldots, \gamma_m]$ such that $\gamma_1 + \cdots + \gamma_m = 1$. From the m estimates ω_N^i of ω by using the m sensor thresholds, their convex combination is also

an estimate $\widehat{\omega}$ of ω

$$\widehat{\omega} = \sum_{i=1}^{m} \gamma_i \omega_N^i = \gamma^T W_N,$$

where $W_N = [\omega_N^1, \ldots, \omega_N^m]$. $\widehat{\omega}$ is called a Quasi-Convex Combination Estimator (QCCE). When the weighting values are selected optimally, we have the optimal QCCE, see [93].

The optimization algorithm is described below. Let ω_N^i, $i = 1, \ldots, m$ be m asymptotically unbiased estimators of ω based on samples of size N. Then the estimation error is defined by $e_N^i = \omega_N^i - \omega$ for each $i = 1, \ldots, m$. The error vector can be expressed as $e_N = \omega_N - \omega \mathbb{1}$ where $\mathbb{1} = [1, 1, \ldots, 1]^T$. Define the covariance matrix of e_N as $V_N = E[e_N e_N^T]$.

Theorem 3 *Suppose that $V_N(\omega)$ is positive definite. Then the optimal QCCE is obtained by choosing*

$$\gamma^* = \frac{V_N^{-1}(\omega)\mathbb{1}}{\mathbb{1}^T V_N^{-1}(\omega)\mathbb{1}}.$$

The minimal variance is

$$\sigma_N^2 = \frac{1}{\mathbb{1}^T V_N^{-1}(\omega)\mathbb{1}}.$$

Proof: Here, we only outline the main steps of the proof. The detailed proof can be found in [93]. Consider the Hamiltonian $H(\gamma, \lambda) = \gamma^T V_N(\omega)\gamma + \lambda(1 - \gamma^T \mathbb{1})$, where λ is the Lagrange multiplier. Using the standard techniques in optimization yields the minimum point γ^* and σ_N^2. □

One way to implement the QCCE numerically is as follows:

- Step 1: Find the sample mean of all estimated values $\widehat{\omega}$, computed from the m-thresholds. The sample mean is

$$\bar{W}_N = \sum_{j=1}^{N} W_j/N.$$

- Step 2: Find the sample covariance $\widehat{V}_N$. The sample covariance is

$$\widehat{V}_N = \frac{1}{N-1}\sum_{j=1}^{N}(W_j - \bar{W}_N)(W_j - \bar{W}_N)^T.$$

- Step 3: Find γ_N as

$$\gamma_N = \frac{\widehat{V}_N^{-1}\mathbb{1}}{\mathbb{1}^T\widehat{V}_N^{-1}\mathbb{1}}.$$

- Step 4: Find $\widehat{\omega}_N = (\gamma_N)^T W_N$.

This algorithm can also be implemented recursively as follows.

$$\begin{aligned}
\bar{W}_N &= \bar{W}_{N-1} - \frac{1}{N}\bar{W}_{N-1} + \frac{W_N}{N} \\
\widehat{V}_N &= \widehat{V}_{N-1} - \frac{1}{N-1}\widehat{V}_{N-1} + \frac{(W_N - \bar{W}_N)(W_N - \bar{W}_N)^T}{N-1}.
\end{aligned}$$

It can be shown [93] that

$$\widehat{V}_N(\omega) - V_N(\omega) \to 0, \quad N \to \infty.$$

To study the efficiency of the QCCE estimator, we compare the variance of this estimator to the CR lower bound. For $i = 1, \ldots, m+1$, define

$$\begin{aligned}
p_i(\omega) &= P\{s_k(i) = 1\} \\
&= P\{C_{i-1} < y_k \leq C_i\} \\
&= F(C_i - \omega) - F(C_{i-1} - \omega) \\
&:= \tilde{F}(\omega).
\end{aligned}$$

Let $h_i(\omega) = \partial p_i(\omega)/\partial\omega = -f(C_i - \omega) + f(C_{i-1} - \omega)$, where $f(\cdot)$ is the probability density function. Then, the sensitivity of ω with respect to p_i is $\partial\omega/\partial p_i = 1/h_i(\omega)$.

Denote

$$h(\omega) = [h_1(\omega), h_2(\omega), \ldots, h_{m+1}(\omega)]^T$$

$$p(\omega) = [p_1, p_2, \ldots, p_m]^T$$

$$U(\omega) = \text{diag}(1/h_1, 1/h_2, \ldots, 1/h_m)$$

$$M(\omega) = \text{diag}(p)$$

$$\Psi(\omega) = U(M - pp^T)U.$$

Let $Q = M^{1/2} = \text{diag}(\sqrt{p_1}, \ldots, \sqrt{p_m})$. M is invertible since p is non-zero and positive. If p_j is zero, the threshold C_j can be eliminated and the interval (C_{j-1}, C_j) does not contain useful information.

Lemma 1 *[93] The Cramèr-Rao lower bound for estimating ω based on observations of s_k is given by:*

$$\sigma^2_{CR}(N, m) = \left(N \sum_{i=1}^{m+1} \frac{h_i^2}{p_i} \right)^{-1}.$$

Theorem 4 *The optimal QCCE is asymptotically efficient in the sense that*

$$N\sigma_N^2 - N\sigma^2_{CR}(N, m) \to 0, N \to \infty.$$

Proof: The variance of the optimal QCCE satisfies

$$\sigma_N^2 = N \frac{1}{\mathbb{1}^T V_N^{-1}(\omega)\mathbb{1}} \to \frac{1}{\mathbb{1}^T \Psi^{-1}(\omega)\mathbb{1}}, N \to \infty,$$

where $\Psi^{-1}(\omega)$ is the limit of $N^{-1}V_N^{-1}(\omega)$. Now from Lemma 1,

$$N\sigma^2_{CR}(N, m) = \left(\sum_{i=1}^{m+1} \frac{h_i^2}{p_i} \right)^{-1}.$$

This leads to $\mathbb{1}^T \Psi^{-1}(\omega)\mathbb{1} = \sum_{i=1}^{m+1} \frac{h_i^2}{p_i}$. □

4.3.2 Examples

In the following examples, we consider the same system and apply the same input as in Example 2. The sensor has four thresholds $115, 122, 130, 135$. Example 5 demonstrates identification accuracy when each threshold is used individually like a binary sensor.

Example 5 We consider the same system as in Example 2, with a fixed noise standard deviation $\sigma = 4$, and the observation length $N = 5000$, but with different threshold values. The results are shown in Table 4.

Table 4: Parameter Estimation by Using The Data of Example 5

Para.	Actual	Estimate C = 115	Estimate C = 122	Estimate C = 130	Estimate C = 135
a_1	-1.0078	-0.8509	-0.8777	-0.8853	-0.9398
a_2	0.2513	0.0252	0.136	0.2241	0.2891
b_1	0.0815	0.0948	0.0901	0.1093	0.0909
b_2	0.0514	0.0481	0.0395	0.0551	0.0571
TSE	-	0.07593	0.03044	0.01653	0.00617

Example 6 We now combine the 4 estimates in Example 5 by using the QCCE algorithm. The measurement noises are i.i.d. Gaussian noise sequences with zero mean and standard deviation $\sigma = 30$. The results are shown in Table 5. Figure 11 compares the estimated speeds of PMDC motor by using each threshold individually with the optimal QCCE by using the combined 4-thresholds. Figure 12 shows the

convergence of the QCCE and convergence rates. Figure 13 compares the sample variance and the theoretical CR bound.

Table 5: Parameter Estimation by Using the Optimal QCCE of 4-Thresholds

Para.	Actual	Estimate N=1000	Estimate N=2000	Estimate N=3000	Estimate N=4000
a_1	-1.0078	-0.8209	-1.1398	-1.0271	-1.009
a_2	0.2513	0.0625	0.3891	0.2558	0.262
b_1	0.0815	0.0948	0.0909	0.0775	0.0863
b_2	0.0514	0.0481	0.045	0.0473	0.04432
TSE	-	0.07077	0.03654	0.00043	0.00019

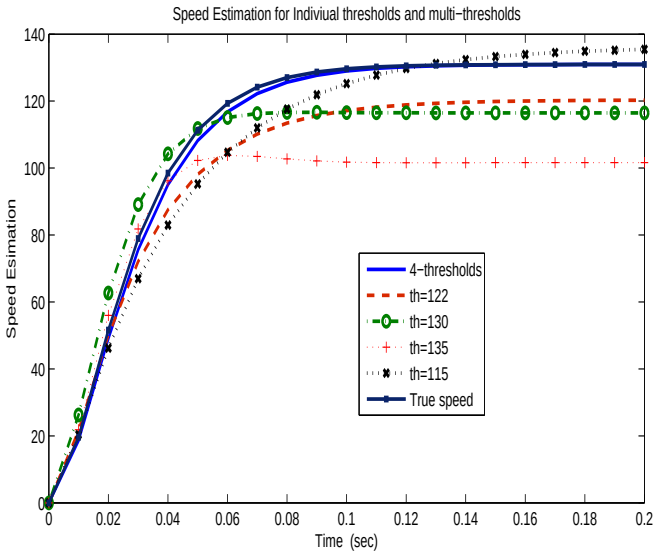

Figure 11: *Speeds of the PMDC motor*

Discussions:

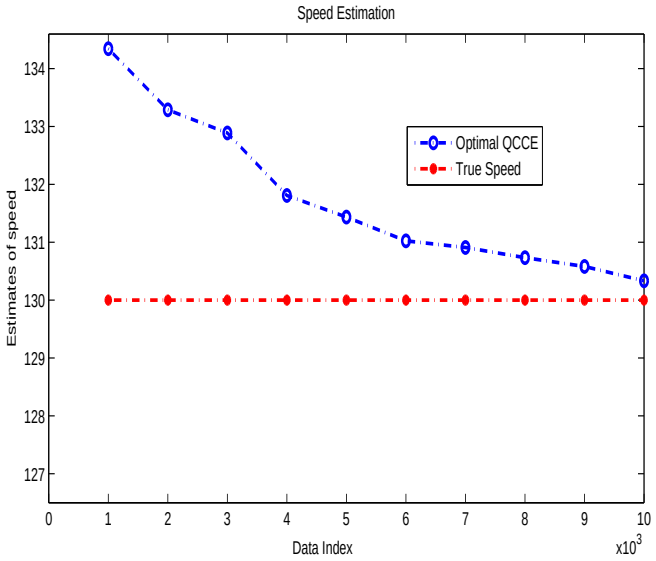

Figure 12: *Convergence of the QCCE and convergence rates*

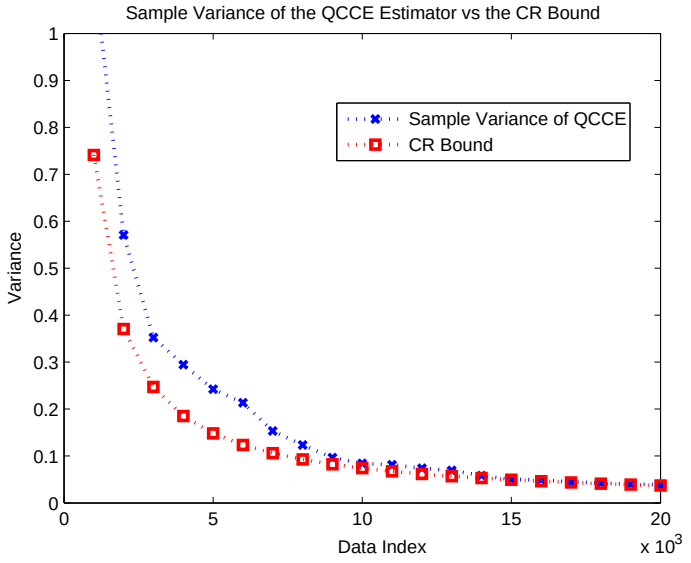

Figure 13: *Sample variance of the QCCE estimator vs. the CR lower bound*

- From Tables 4, 5, and Figure 11, one can see that using multi-thresholds in parameter estimation is quite effective, because the TSE errors between the actual and estimated parameters decrease significantly. Also it is noted that the observation length using multi-thresholds can be shorter than that for the single threshold. Even if higher standard deviations are used in the case of multi-thresholds ($\sigma = 30$ in Example 6 vs. $\sigma = 4$ in Example 4), identification accuracy is sustained.

- From Figures 12 and 13, it can be seen that using the optimal QCCE is an effective method that improves convergence rates towards the CR bound.

- The above observations highlight some practical guidelines in selecting some design variables: (1) Choose N based on the CR lower bound so that the corresponding estimation errors fall within tolerance specifications. The sample variance will be close to it. (2) If the desired motor speed is near a constant, the thresholds of the quantizer can be pre-optimized by using the CR lower bound.

4.4 Experimental Verification

This section presents experimental verification of our algorithms. The main equipment and measurement devices for the experimental platform include: (1) The Renesas DC Motor Control Demonstration Kit (YMCRPR8C25). This combined testing/demo motor control system consists of the following subsystems: YMCRPR8C25 motor control board; a PMDC motor with specifications 24 V/0.5 A power rating and rated speed 4000 rpm; and an AC Adapter, 24 VDC 5A, center positive. (2) The NI SCB-68 shielded I/O connector block for interfacing I/O signals to plug-in data acquisition (DAQ) devices with 68-pin connectors. Combined with the shielded cables, the SCB-68 provides rugged, very low-noise signal termination. It is compatible with single- and dual-connector NI X Series and M Series devices with 68-pin connectors. The connector block is also compatible with most NI E, B, S, and R Series DAQ devices. (3) A desktop computer which has LabVIEW software installed (ver 2011), (4) A digital multimeter. The devices are connected into a testing platform, shown in Figure 14 for the motor control kit and Figure 15 for the integrated test platform.

Motor input voltage is controlled from the LabVIEW software on the desktop computer, but also measured at the motor. Motor speeds are physically measured at the motor by a Hall-effect sensor. Using two channels of data acquisition, the measurement data on the input and speed are fed into the computer by using the data acquisition software of the motor control kit and then imported to the Labview platform. Random dithers are added to the data and then passed through a quantized

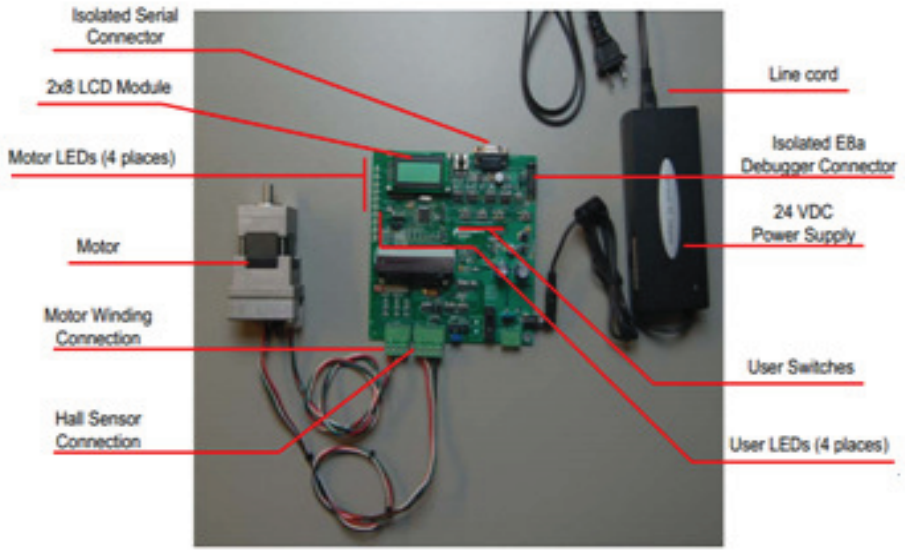

Figure 14: *The motor control and evaluation kit*

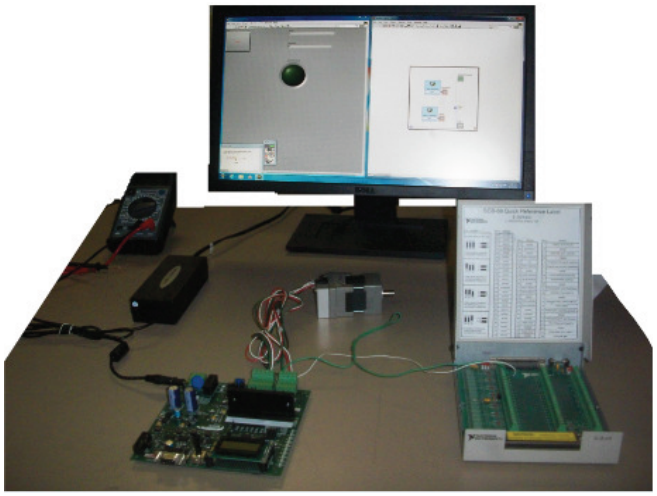

Figure 15: *The experimental verification system*

sensor of selected thresholds. The data on the input voltage and motor speed are sampled values. The data are collected in real time, then stored using Microsoft Excel 2007. Typical segments of the data are shown in Figure 16 on the input voltage and in Figure 17 on the motor speed. We should clarify that due to a hardware limitation which does not allow synchronized real-time data acquisition and parameter estimation, the data are collected in real time, saved, and then used in estimation. Since parameter estimation is an open-loop operation, this limitation does not affect the results.

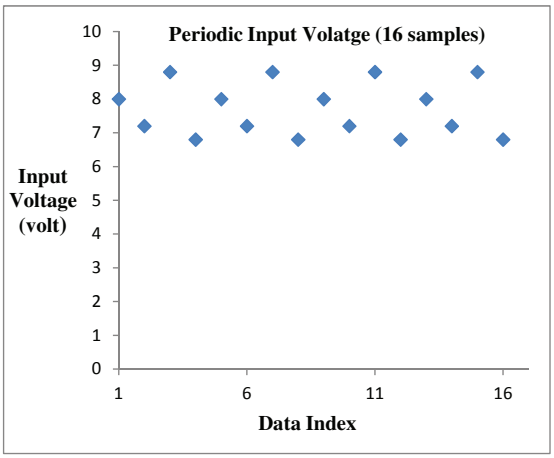

Figure 16: *Periodic input voltage profiles*

Example 7 The sampling interval is selected as $T = 0.01$ sec. The input voltage is a 4-periodic function with amplitudes shown in Fig. 16. The motor specification values as supplied by the manufacturer are as follows: $L_a = 0.0023$ H, $R_a = 1.68$ ohm, $J = 0.0011\ Kg.m^2$, $\mu = 9.8 \times 10^{-8}\ N.m.s$, $k_m = k_b = 0.033\ N.m/A$ or $V/rad/s$. The added measurement dithers are i.i.d. Gaussian random sequences

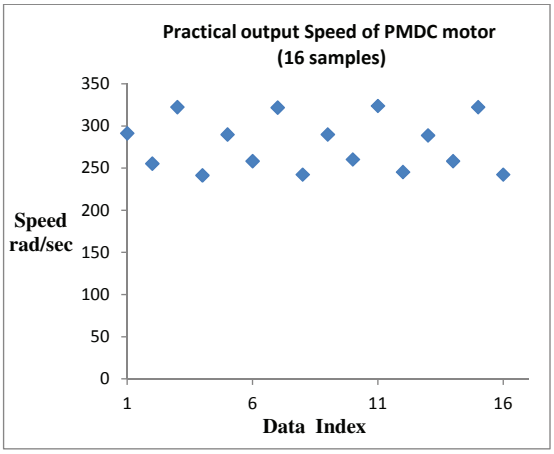

Figure 17: *Periodic output speeds of the PMDC motor*

with zero mean and standard deviation $\sigma = 25$. Under quantized measurements with thresholds $C_1 = 245, C_2 = 278, C_3 = 295, C_4 = 318$, $N = 10000$ samples are collected. By using the QCCE estimator, the parameter estimates are summarized in Table 6. To evaluate the estimation accuracy, the sample variances of the estimation error sequences are compared to theoretically computed CR lower bound under the given motor parameters and testing conditions. Figure 18 shows the sample variance trajectory of the QCCE estimator and the theoretical CR lower bound.

Table 6: QCCE Estimation Using the Experimental Data of Example 7

Parameter	Actual	Estimated
a_1	-0.9939	-0.9709
a_2	6.7203e-4	6.25e-4
b_1	0.1538	0.1639
b_2	0.0929	0.0969
TSE	-	0.00065

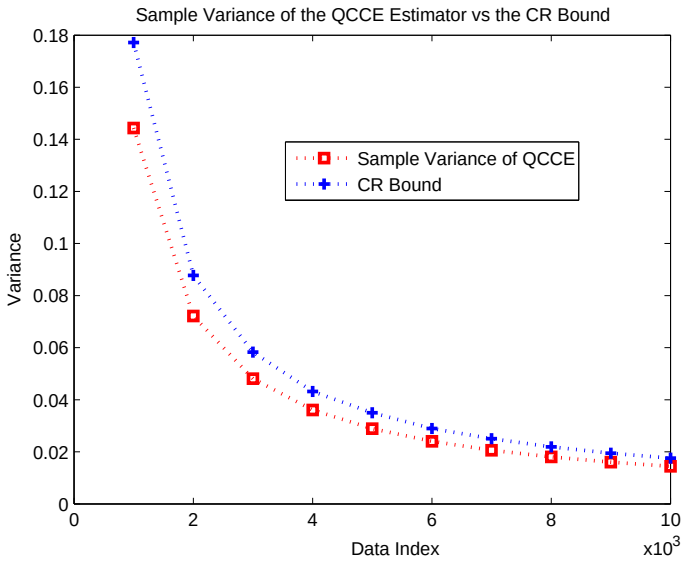

Figure 18: *Sample variance trajectory of the QCCE estimator vs the CR bound*

Chapter 5 SIGNAL ESTIMATION AND CLOSED-LOOP SYSTEM PERFORMANCE OF PMDC MOTORS WITH COMMUNICATION CHANNELS

This chapter investigates unique issues rising from feedback control of electric motors with embedded communication channels [89]. For concreteness, PMDC motors are employed as a representative system for carrying out our analysis and simulation, although the findings of this chapter are applicable to other motor types.

To characterize impact of the above-mentioned design variables on motor control, we focus on several commonly used performance measures. It is well understood that the feedback mechanism provides some critical functions: (1) Transient performance.

This is typically specified by the step response and its characterizing parameters such as the rise time, settling time, peak time, and overshoot. (2) Tracking capability. When the command signals are time varying, the motor speed must follow them quickly and accurately. We will use the ramp and sinusoid inputs as testing commands for the tracking aspect of the motor system. (3) Disturbance attenuation. Measurement errors and communication uncertainties are represented by noises. They cause the motor speed to fluctuate. It is important that the feedback system can attenuate such disturbances on the motor speed. These will be used to evaluate relations between key design variables and motor performance.

To compare to the standard computer-controlled system without communications, we note that in classical digital control design, one designs a continuous-time controller first. Then the controller is discretized after choosing a sampling interval. Usually, as long as the sampling interval is sufficiently small, the sampled system will deliver a similar performance to the continuous-time controller. Communication channels depend on network traffic conditions and deliver different throughput, implying that the sampling intervals may change. Since signal estimation is updated on the arrival of new data, its dynamics actually change with the sampling interval. Consequently, interaction among sampling, signal estimation, and the controller will introduce new issues in remotely controlled motors.

Our results will demonstrate that many components of design variables interact closely to determine feedback properties. These include sampling interval, quantization levels, signal estimation data windows, motor dynamics, controllers, and signal

estimation algorithms. The theoretical foundation for analyzing such systems was first introduced in [42, 43] under a simplified loop structure. Employing PMDC motors as a platform, this chapter treats a remotely controlled motor with two communication channels, one from the motor speed measurement to the remote controller, and the other from the remote controller to the motor voltage input for the feedback control signal. These two channels may have different sampling periods and signal estimation schemes, leading to an asynchronous framework which is more flexible than the commonly-employed synchronous sampling schemes.

The rest of the chapter is organized as follows. Section 5.1 described the system configuration of closed loop feed back PMDC system interact with communication channels. Then Section 5.2 introduces the main algorithms for signal estimation. Typical and optimal signal estimation schemes can be represented by a signal averaging filter with its time constant derived from the step size of the signal estimation algorithm. To evaluate interactions of the feedback system, signal filter parameter, and sampling interval, Section 5.3 presents some case studies covering a variety of scenarios. They clearly indicate that these parameters must be carefully chosen to retain feedback performance. From these cases, we highlight some design guidelines so that motor operations can deliver desired performance robustly.

5.1 Feedback Systems with Communication Channels

In order to understand the effect of adding one or two communication blocks and signal estimation algorithms, we will first study system performance without commu-

nication blocks. These will serve as performance references when evaluating impact from communications and signal estimation algorithms. All simulations in this dissertation use Matlab/Simulink codes.

Example 8 Suppose that a PMDC motor has the following parameters (from the manufacturer): $L_a = 0.02$ H, $R_a = 2.0$ ohm, $J = 0.07\ Kg.m^2$, $\mu = 0.045\ N.m.s$, $k_p = k_m = 2.5\ N.m/A$ or $V/rad/s$. The system is sampled with the sampling period $T_s = 0.01$ second. In an open-loop environment (without the PI controller), Figure 19 shows the step responses of the original continuous-time model and its sampled system. It is clear that the sampling interval is adequate for the sampled system to approximate the original continuous-time system. Figure 20 illustrates the step responses when the the PI controller is applied, with the continuous-time PI expression for the continuous-time plant and the discrete-time PI controller for the sampled system. Apparently, feedback controller improves motor performance and the sampling interval remains suitable.

To further demonstration of performance, Figures 21 and 22 present the ramp and sinusoid responses of the closed-loop system with the PI controller. In all above cases, we observe that without communication links, the controller performs well in terms of stability and performance. Also, the discretized models are sufficiently accurate as approximations for system identification and control, indicating that the sampling interval $T_s = 0.01$ is adequate.

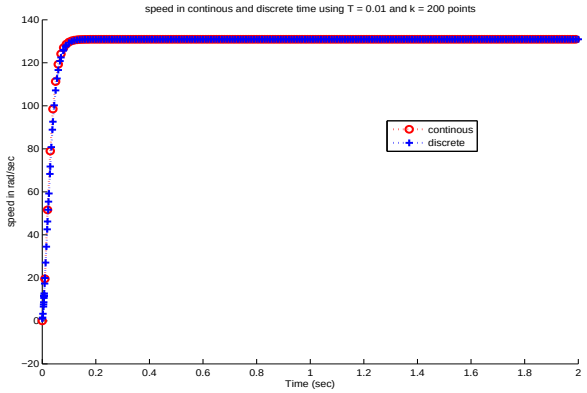

Figure 19: *Step response of PMDC motor in open loop (without the controller)*

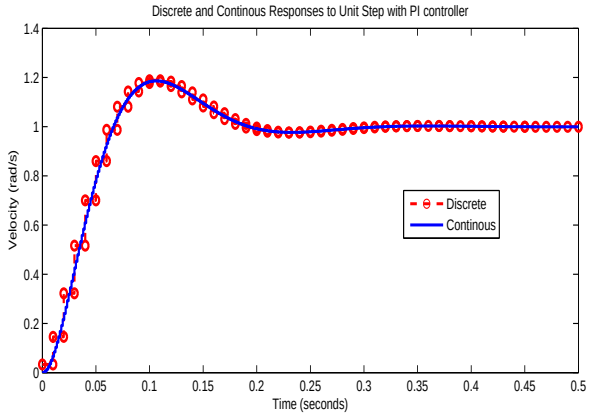

Figure 20: *Step response of PMDC motor in closed loop (with the controller)*

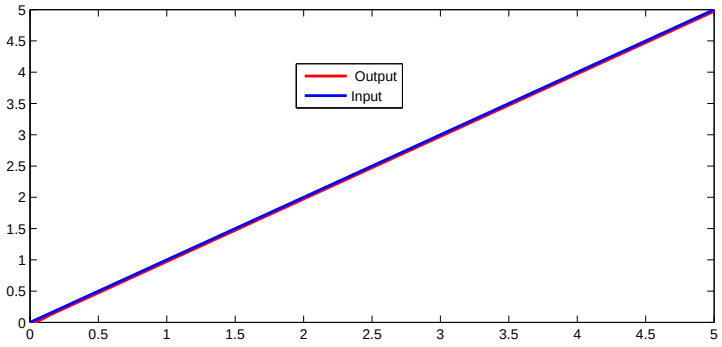

Figure 21: *Ramp response of the closed-loop system with the PI controller*

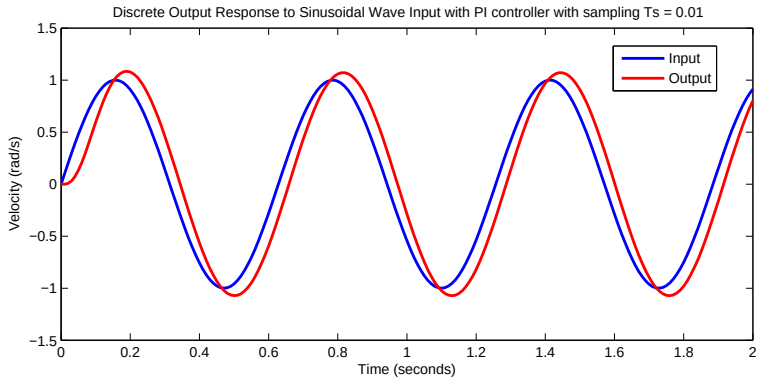

Figure 22: *Sinusoid response of the closed-loop system with the PI controller*

When a PMDC motor must be remotely controlled, communication channels are inserted into the feedback loop, leading to a new system structure shown in Figure 23. The overall system consists of the PMDC motor transfer function G(z), the PI controller C(z), communication blocks in both output and input sides. In this configuration, the output speed signal $\omega(t)$ and the control signal u_k are communicated through communication channels, and then estimated. In our development, we allow the two communication blocks and signal estimation algorithms to have different sampling intervals and step sizes, in order to accommodate realistic wireless communication networks.

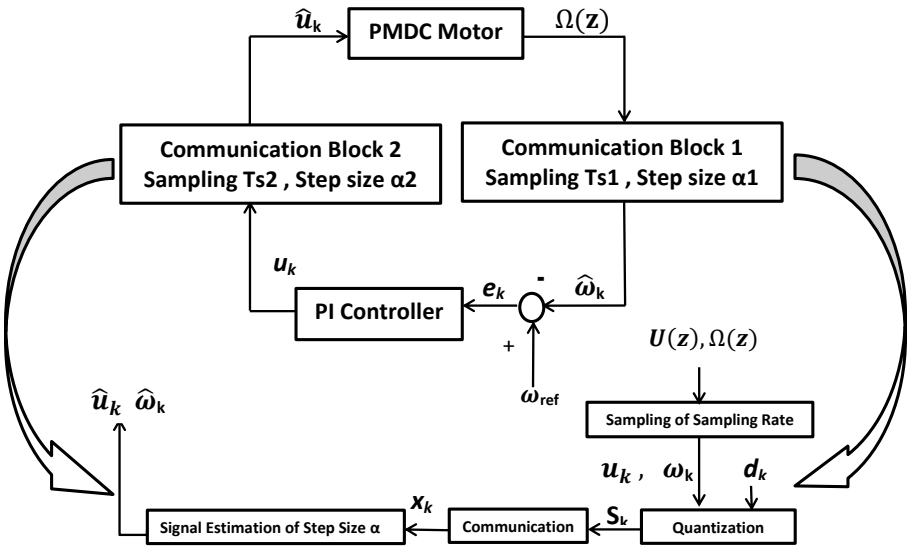

Figure 23: *Closed-loop PMDC system with communication channels*

Inserting a communication block to transmit a signal in the feedback loop introduces some errors; and signal estimation leads to dynamic delays. In this dissertation we aim to study the behavior of the PMDC closed-loop system under the commu-

nication channels and signal estimation algorithms by analyzing interactions among quantization, sampling, signal estimation, and feedback stability and performance of PMDC motors. We will also show that there are certain fundamental issues that an engineer must consider when designing remotely controlled PMDC motors.

5.2 Communication Channels and Signal Estimation

When signals must be transmitted through communication channels, they are sampled, quantized, and transmitted; then recovered and estimated at the receiving side [89]. Signal averaging methods are commonly used in such signal recovery schemes to reduce errors and noises on the signals. This is especially true under lower-precision quantization schemes.

In principle, low-precision quantization, such as binary-valued quantization, will not transmit sufficient information on the signals for feedback control. However, by employing the smoothing effects of random noises or dithers, more information can be recovered, see [41, 42] comprehensive exploration of related algorithms and properties. It was shown in [42] that the algorithms that extract information on the original signals act like averaging filters that introduce new dynamics into the feedback loop. Consequently, they affect feedback stability and performance.

The methodology we used here was initially developed in [42, 43] with one block representing lumped communication channels. In this dissertation two communication blocks are used: one to transmit and estimate the motor output speed signal to the controller and the other to transmit and estimate the controller output signal

back to the motor. This is a challenging problem since signal averaging algorithms interact with sampling and quantization of the communication channels and affect the feedback system's performance. The main question is: What is the behavior of the closed-loop system under these two channels and signal estimation algorithms?

In the subsequent performance evaluations, we will employ the step responses in which the standard performance measures are the rise time t_r, settling time t_s, peak time t_{max}, and percentage overshoot M_p, see [92] for their definitions. Within these measures, the rise time and peak time represent response speeds; the overshoot represents control accuracy; and the settling time represents control effective duration. All these parameters are desired to be small.

5.2.1 PMDC Signal Estimation

We now explain the methodology of signal estimation which was introduced in [42, 43], and some essential derivation steps that will be relevant in our study. We will use the output speed signal ω_k in describing the algorithms and main features. The estimation steps and features for the control signal u_k will be similar.

The true motor speed ω_k is bounded in $\omega_{min} \leq w_k \leq \omega_{max}$. ω_k is either measured with a measurement noise or added with a random dither d_k to enhance signal estimation.

The noise-added signal $\omega_k + d_k$ is quantized to produce a quantization sequence $s_k = \mathcal{S}(\omega_k + d_k)$, where $\mathcal{S}$ represents the quantization function. More precisely, suppose that the signal $\omega_k + d_k$ is quantized by m quantization thresholds $\{h_1, \ldots, h_m\}$, which divides the range $[\omega_{\min}, \omega_{\max}]$ into $\omega_{\min} < h_1 < \cdots < h_m < \omega_{\max}$. The output of the quantizer takes $m+1$ possible values $\{1, 2, \ldots, m+1\}$ and is represented by

$$s_k = \sum_{i=1}^{m+1} i I_{\{h_{i-1} < \omega_k + d_k \leq h_i\}} \tag{5.16}$$

with $h_0 = 0$ and I being the indicator function. In the special case of a binary-valued quantization of threshold h,

$$s_k = \begin{cases} 1, & \text{if } \omega_k + d_k \leq h, \\ 0, & \text{if } \omega_k + d_k > h. \end{cases}$$

For clarity, we will use the binary-valued quantization to derive algorithms and properties. Generalization to m quantizion levels can be found in [42]. s_k will be processed to estimate ω_k at the receiver side.

Signal Estimation Algorithms:

For a selected $0 < \alpha < 1$, define the following truncated and exponentially weighted empirical measures

$$\zeta_k^\nu = (1-\alpha)\sum_{l=-\infty}^{k} \alpha^{k-l} s_l, \tag{5.17}$$

where the weight is normalized so that when $s_l \equiv 1$, $(1-\alpha)\sum_{l=0}^{\infty}\alpha^l = 1$. This algorithm can also be written recursively as

$$\zeta_k^\nu = \zeta_{k-1}^\nu + (1-\alpha)(s_k - \zeta_{k-1}^\nu) = \zeta_{k-1}^\nu + \beta(s_k - \zeta_{k-1}^\nu),$$

which is a stochastic approximation algorithm with a constant step size $\beta = 1-\alpha$.

To understand the meaning of the weight α and the step size $\beta = 1-\alpha$, we note that (5.17) is a weighted averaging computation. The smaller the α value, the faster the decaying rate α^{k-l} in (5.17), which in turn implies the averaging uses mostly the recent data, that is a small data window in the sinal averaging. This is equivalent to β being close to 1. This represents a fast updating algorithm. Such an algorithm will be able to track fast changing signals, but will have less capability in attenuating noise effects. However, this is a fast response filter (i.e., less dynamic delay) and hence will have less detrimental effects on feedback stability and performance. This intuitive understanding will help in interpreting case study results.

In addition, when we translate the step sizes to the actual time, each updating step in signal estimation means T_s second. Consequently, the sampling period is a fundamental parameter when feedback performance is evaluated.

For a technical delicacy, for some small δ satisfying $0 < \delta < 1$, define

$$\zeta_k = \begin{cases} \zeta_k^\nu, & \text{if } \delta < \zeta_k^\nu < 1-\delta; \\ \delta, & \text{if } \zeta_k^\nu < \delta; \\ 1-\delta, & \text{if } \zeta_k^\nu > 1-\delta. \end{cases} \tag{5.18}$$

This will not affect system analysis. Then, the estimation of ω_k is

$$\widehat{\omega}_k = h - F^{-1}(\zeta_k). \tag{5.19}$$

5.2.2 Filter Representation and Error Analysis

It can be shown [42] that adding the signal estimation algorithm (5.19) into the PMDC feedback loop can be represented by a signal averaging filter and an equivalent noise source. Consequently the block diagram of the closed loop PMDC is expanded with two filters $H_{\alpha 1}(z) = \frac{(1-\alpha_1)z}{z-\alpha_1}$ and $H_{\alpha 2}(z) = \frac{(1-\alpha_2)z}{z-\alpha_2}$, shown in Figure 24.

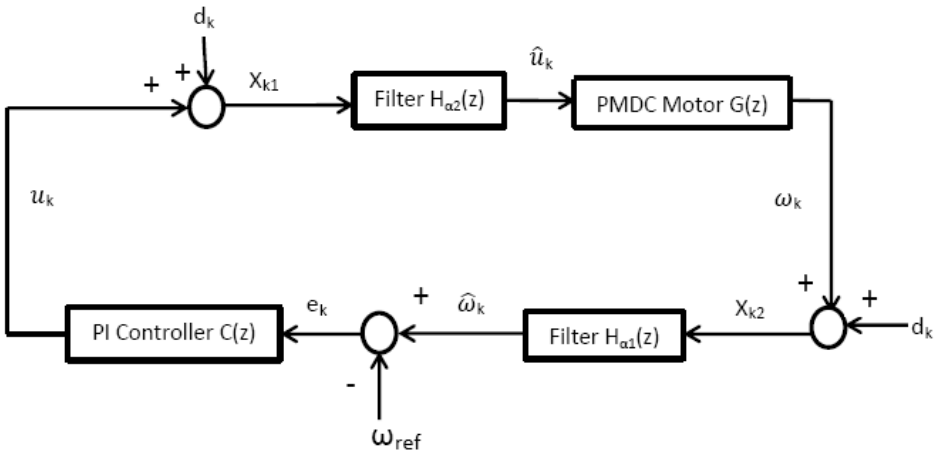

Figure 24: *Simplified equivalent system*

The following property, established in [43], establishes a convergence property for

this filter representation.

Lemma 2

$$\lim_{\alpha\to 1} E\widehat{\omega}_k = \theta \quad \text{and} \quad \lim_{\alpha\to 1} \frac{1+\alpha}{1-\alpha} E(\widehat{\omega}_k - \theta)^2 = \frac{F(h-\theta)(1-F(h-\theta))}{f^2(h-\theta)}. \tag{5.20}$$

This Lemma implies that asymptotically, $\widehat{\omega}_k = \omega_k + \delta_k$, where the estimation error δ_k satisfies $E\delta_k = 0$ and $E\delta_k^2 = \frac{1-\alpha}{1+\alpha}\frac{F(h-\theta)(1-F(h-\theta))}{f^2(h-\theta)}$. Here we note that by [93], $F(1-F)/(Nf^2)$ is the CR lower. In this sense, Lemma 2 establishes that the algorithm (5.18) achieves the CR lower bound asymptotically, and hence is asymptotically efficient when $\alpha \to 1$.

On the other hand, the same characterization may be derived from a filter

$$H_\alpha(z) = \frac{(1-\alpha)z}{z-\alpha} \tag{5.21}$$

that acts on $\omega_k + d_k$ with $\{d_k\}$ being a sequence of i.i.d. random variables satisfying

$$Ed_k = 0 \quad \text{and} \quad \sigma_d^2 = Ed_k^2 = \frac{F(h-\omega_k)(1-F(h-\omega_k))}{f^2(h-\omega_k)}.$$

Indeed, suppose $x_k = \omega_k + d_k$ and $\omega_k = \theta$ is a constant. Let $z_k = Fx_k$, namely $z_k = (1-\alpha)\sum_{l=-\infty}^{k} \alpha^{k-l} x_l$. Then $Ez_k = \theta$ and

$$E(z_k - \theta)^2 = (1-\alpha)^2 \sum_{l=0}^{\infty} \alpha^{2l}\sigma_d^2 = \frac{1-\alpha}{1+\alpha}\sigma_d^2. \tag{5.22}$$

In other words, the estimator (5.19) can be simply represented by the filter $H_\alpha(z)$ with an equivalent noise d_k in Figure 24. The step size of the algorithm determines the filter time constant.

5.2.3 Impact of Signal Estimation on Feedback Performance

Now, suppose we add only a communication block 1 to the system. Consider a feedback system shown in Figure 24 whose open-loop system $P(z)$, which combines the controller and plant, has a minimal state space realization

$$P(z): \quad \begin{cases} x_{k+1} &= Ax_k + Bu_k \\ \omega_k &= Cx_k. \end{cases} \tag{5.23}$$

It is assumed that the closed-loop system under the negative unity feedback $u = -\omega_k$ is stable.

For a (sufficiently small) sampling interval T_{s1}, the overall closed-loop system with signal estimation on ω_k becomes

$$\begin{aligned} x_{k+1} &= x_k + T_{s1}(Ax_k + Bu_k) \\ \omega_k &= Cx_k \\ s_k &= \begin{cases} 1, & \omega_k + d_k \le h \\ 0, & \omega_k + d_k > h \end{cases} \\ \xi_{k+1} &= \xi_k + \beta(s_k - \xi_k) \\ \widehat{\omega}_k &= h - F^{-1}(\xi_k) \\ u_k &= -\widehat{\omega}_k. \end{aligned} \tag{5.24}$$

Theorem 5 *Suppose that the sampling interval T_{s1} is proportional to the step size β: $T_{s1}/\beta = \lambda$. Then, the closed-loop system is*

$$\begin{cases} x_{k+1} &= x_k + T_{s1}(A_0 x_k - B(\gamma - F^{-1}(\xi_k) - Cx_k) \\ \xi_{k+1} &= \xi_k + \frac{1}{\lambda} T_{s1}(s_k - \xi_k). \end{cases} \tag{5.25}$$

Proof: Define the signal estimation error $e_k = \widehat{y}_k - y_k$. The state equation can be modified to

$$x_{k+1} = x_k + T_{s1}(Ax_k - B\widehat{y}_k) = x_k + T_{s1}(Ax_k - B(y_k + e_k)) = x_k + T_{s1}((A - BC)x_k - Be_k).$$

Hence, we have

$$\begin{cases} x_{k+1} &= x_k + T_{s1}(A_0 x_k - Be_k) \\ \xi_{k+1} &= \xi_k + \beta(s_k - \xi_k). \end{cases}$$

Since $e_k = \gamma - F^{-1}(\xi_k) - Cx_k$, we have (5.25). □

Theorem 6 *As $T_{s1} \to 0$, $(x^{T_{s1}}(\cdot), \xi^{T_{s1}}(\cdot))$ converges weakly to $(x(\cdot), \xi(\cdot))$ such that $(x(\cdot), \xi(\cdot))$ is a solution of the ordinary differential equation*

$$\begin{cases} \dot{x} = A_0 x - B(\gamma - F^{-1}(\xi) - Cx) \\ \dot{\xi} = \dfrac{1}{\lambda}(F(\gamma - Cx) - \xi), \end{cases} \tag{5.26}$$

provided that (5.26) *has a unique solution for each initial condition.*

The unique equilibrium point of (5.26) is $\xi = F(\gamma)$ and $x = 0$. We further derive the locally linearized system of (5.26) at the equilibrium point.

Theorem 7 *The locally linearized system of (5.26) is*

$$\dot{x} = Ax + Bu, \quad \omega = Cx, \quad \dot{u} = -\frac{1}{\lambda}\omega - \frac{1}{\lambda}u, \tag{5.27}$$

which is exactly the feedback system with

$$\omega = P(s)u, \ u = -R(s)\omega, \tag{5.28}$$

where $R(s) = \frac{1}{\lambda s + 1}$.

Proof: Since $\lambda \neq 0$ and, as a stable matrix, A_0 is non-singular, the equilibrium point of (5.26), solved from

$$\xi = F(\gamma - Cx), \quad \lambda A_0 x = 0,$$

is unique $\xi = F(\gamma)$, $x = 0$. Define $v = \xi - F(\gamma)$. For stability analysis, we may transform the limit system (5.26) into a system of x and v, with the equilibrium point $x = 0$ and $v = 0$,

$$\begin{cases} \dot{x} = A_0 x - B(\gamma - F^{-1}(v + F(\gamma)) - Cx) \\ \dot{v} = \dfrac{1}{\lambda}(F(\gamma - Cx) - F(\gamma) - v). \end{cases} \tag{5.29}$$

The Jacobian matrix of (5.29) at $x = 0$, $v = 0$ is

$$\overline{A} = \begin{bmatrix} A & \frac{B}{f(\gamma)} \\ -f(\gamma)C/\lambda & -1/\lambda \end{bmatrix}. \tag{5.30}$$

Hence, the locally linearized system of (5.29) is

$$\begin{cases} \dot{x} = Ax + \dfrac{B}{f(\gamma)} v \\ \dot{v} = -\dfrac{1}{\lambda} f(\gamma) Cx - \dfrac{1}{\lambda} v. \end{cases} \tag{5.31}$$

Now, by defining $u = v/f(\gamma)$, the linearized system (5.31) becomes (5.27). By (5.23) and after taking the Laplace transform of the last equation, we obtain (5.28). □

Remark 4 The above result establishes a basic relationship

$$\alpha = e^{-T_{s1}/\lambda}. \tag{5.32}$$

When $T_{s1} \to 0$, the filter $H_\alpha(z) = \frac{(1-\alpha)z}{z-\alpha}$ in (5.21) can be approximated by the continuous-time filter

$$R(s) = \frac{1}{\lambda s + 1} \tag{5.33}$$

in the sense that $\max_{t\in[kT_{s1},(k+1)T_{s1})} |\omega(t) - \omega(kT_{s1})| = o(T_{s1})$ where $o(T_{s1})/T_{s1} \to 0$, as $T_{s1} \to 0$. For a simply understanding, note that the $R(s)$ has impulse response $r(t) = \frac{1}{\lambda}e^{-t/\lambda},\ t \geq 0$. Acting on a continuous-time signal $x(t)$, its output is $\omega(t) = \int_{-\infty}^{t} r(t-\tau)x(\tau)d\tau = \frac{1}{\lambda}\int_{-\infty}^{t} e^{-(t-\tau)/\lambda}x(\tau)d\tau$. For small T_{s1}, $\omega(t)$ is approximated by

$$\begin{aligned}\omega_k = \omega(kT_{s1}) &= \frac{1}{\lambda}\int_{-\infty}^{t} e^{-(t-\tau)/\lambda}x(\tau)d\tau = \frac{T_{s1}}{\lambda}\sum_{i=-\infty}^{k}(e^{-T_{s1}/\lambda})^{k-i}x_i + o(T_{s1}) \\ &= \frac{T_{s1}}{\lambda(1-\alpha)}(1-\alpha)\sum_{i=-\infty}^{k}\alpha^{k-i}x_i + o(T_{s1}) = (1-\alpha)\sum_{i=-\infty}^{k}\alpha^{k-i}x_i + o(T_{s1}),\end{aligned}$$

where $\alpha = e^{-T_{s1}/\lambda}$. This is reduced to the filter H_α in (5.21).

The above analysis confirms that for asymptotic analysis of the feedback system with communication channels and signal estimation, the limit ODE is (5.28) and the signal estimation can be represented by a filter $R(s)$. This structure forms the foundation of subsequent system analysis and design. From (5.32), $\lim_{T_{s1}\to 0}\frac{T_{s1}}{(1-\alpha)} = \lambda$. This relationship represents an inherent interaction among sampling interval T_{s1}, signal estimation weight α, and closed-loop stability.

5.3 Case Study 1: Output Communication Block 1 Only

In this section we will study the impact of signal averaging weight α_1 and sampling period T_{s1} after adding one communication block to the closed-loop PMDC motor system. The system performance will be quantitatively analyzed by the step response parameters, and then further illustrated by ramp and sinusoid responses.

5.3.1 Impact of Signal Averaging Weight α_1

In order to study the impact of signal averaging after adding the communication block 1 to the closed-loop PMDC system, we will take different values of α_1 and assess the corresponding responses.

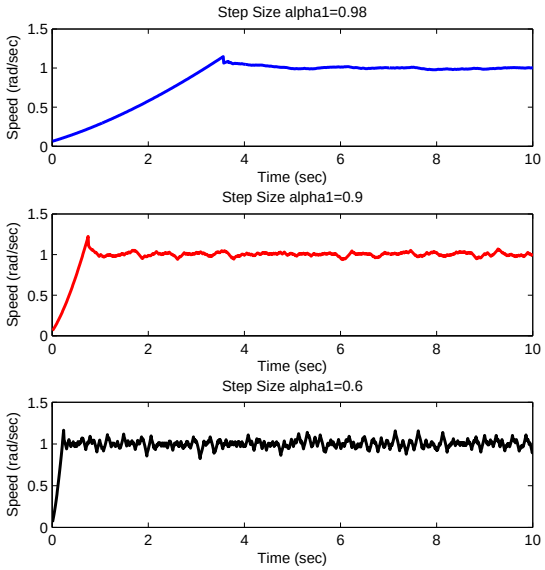

Figure 25: *Effects of signal averaging weights: step response*

Example 9 Consider the same PMDC specifications as in Example 8, but now we add the communication block 1 with the signal estimator (5.19). The estimator can be represented by a filter whose step size is α_1 and sampling interval is T_{s1}. The sampling period is fixed as $T_{s1} = 0.01$. Three values of α_1 are used and their impacts on system performance are compared. Performance evaluations are conducted by using the step, ramp, and sinusoid inputs: Figure 25 for the step response; Figure 26 for the ramp response; and Figure 27 for the sinusoid input.

Table 7: Step Response Performance of Figure 25

α_1	t_r	t_s	t_{max}	M_p
0.98	2.74	5.06	3.56	14.62
0.90	0.57	2.08	0.78	16.54
0.60	0.14	1.50	0.19	17.71

Discussions: From Figure 25, we can derive closed-loop performance parameters in Table 7. We recall that α_1 represents sizes of data window sizes in signal averaging. When α_1 is large (close to 1), see the top plot of Figure 25, the window size is large. This represents a slower dynamics but has more averaging effect. Consequently, the output noise is attenuated, leading to a smooth speed profile. On the other hand, a slow filter dynamics imply slower responses and less aggressive feedback, resulting in smaller overshoot. These are clearly reflected in Table 7: as α_1 increases, t_r, t_s, and t_{max} increase, but the overshoot reduces. This trade-off must be carefully considered when designing motor controllers. In principle, if output noises are small, then small data windows can be used.

In terms of time-varying commands, such as ramp and sinusoid inputs, if α_1 is small, the system has a better tracking capability. This is seen in Figure 26 and Figure 27, especially the bottom plots. The top plots indicate clearly that large α_1 cannot be used if tracking performance is essential since the feedback system cannot follow such command signals.

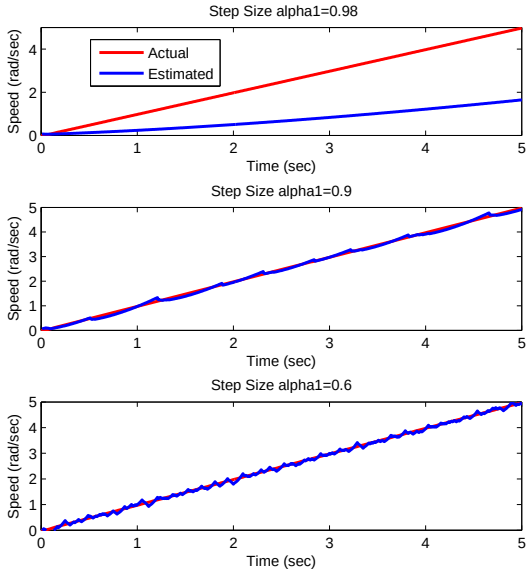

Figure 26: *Effects of signal averaging weights: ramp response*

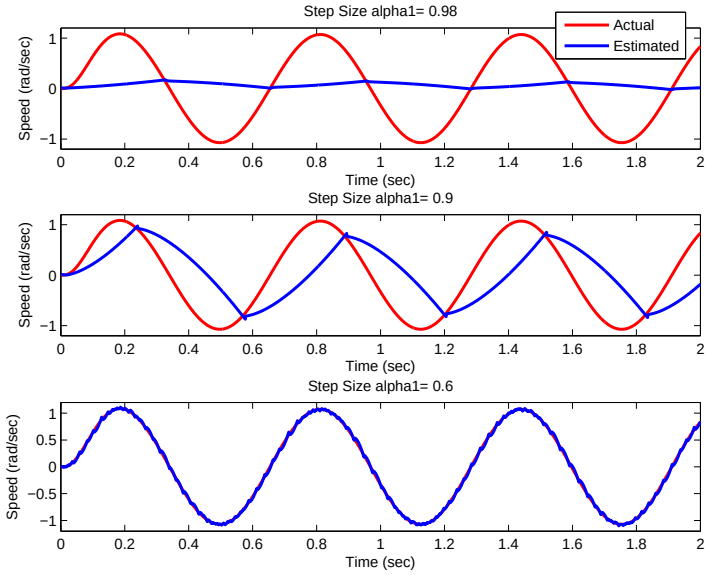

Figure 27: *Effects of signal averaging weights: sinusoid response*

5.3.2 Impact of Sampling Interval T_{s1}

In order to study the impact of sampling rate after adding a communication block 1 to the closed loop PMDC system, we will take different values of T_{s1} and compare closed-loop performances.

Example 10 Consider the same PMDC specifications as in Example 8. In this example the step size of the filter is fixed $\alpha_1 = 0.95$ and three different values of T_{s1} are applied. Then the signal estimator (5.19) is applied for the three cases. Figure 28 shows the step response of the closed-loop PMDC motor under different values of T_{s1}, with performance comparison detailed in Table 8. Figure 29 and Figure 30 demonstrate the output speed responses under the ramp and sinusoid inputs, respectively.

Discussions: It is well understood that in typical sampled-data systems, if the sampling interval is sufficiently small, the sampled system will approximate well the original continuous-time systems, and varying the sampling interval to smaller values will have little impact on such approximations. By observing Figure 28, this is obviously not the case here. When the sampling interval changes, the closed-loop performance is affected significantly. From Table 8, as T_{s1} increases, t_r, t_s, and t_{max} increase, while the overshoot decreases. This effect is similar to Example 9 when α_1 increases.

To understand the significance of this result, consider a typical communication traffic. Due to request priorities and routing congestion conditions, communication

data transmission rates are usually time varying. Our result points out that motor performance will fluctuate significantly along with communication network operations. Consequently, motor control performance becomes un-predictable. The question is: How can we find a remedy for this situation?

By comparing Figures 26 and 29, it is cleared that if α_1 and T_{s1} are tuned collaboratively, then the effect of time-varying T_{s1} can be compensated by the adaptive α_1. In principle, when the sampling interval increases and the weight α_1 should be reduced. The desirable relationship for this step-size adaptation is given by (5.32): for a selected constant λ, α_1 should be adapted according to $\alpha_1 = e^{-T_{s1}/\lambda}$.

The above observation further expand to ramp and sinusoid responses from Figures 27 and 30. We notice that tracking capability improves with smaller T_{s1}. This can also be explained as having the effect of reducing the de factor step size β, leading to a fast tracking ability. But similar to adjustment of α_1, fast tracking capability comes with a price of reduced ability in attenuating noises.

Table 8: Step Response Performance of Figure 28

T_{s1}	t_r	t_s	t_{max}	M_p
0.1	11	16.06	14.70	7.91
0.01	1.10	2.76	1.41	13.13
0.001	0.12	1.16	0.17	17.11

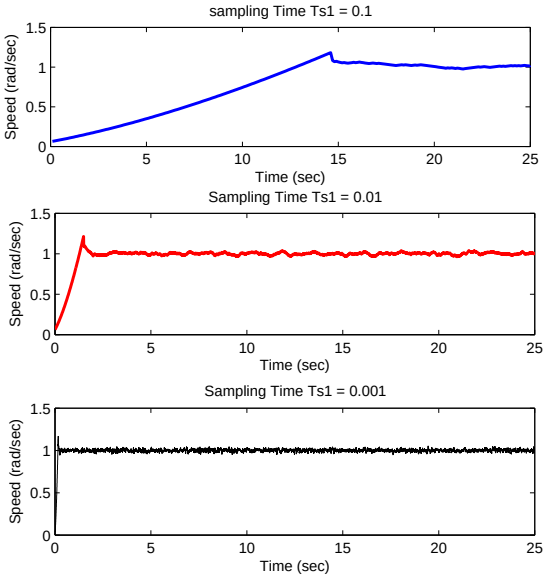

Figure 28: *Effects of sampling intervals: step response*

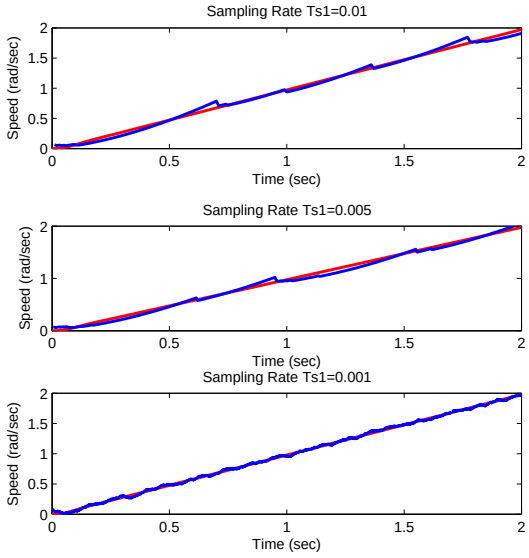

Figure 29: *Effects of sampling rates: ramp response*

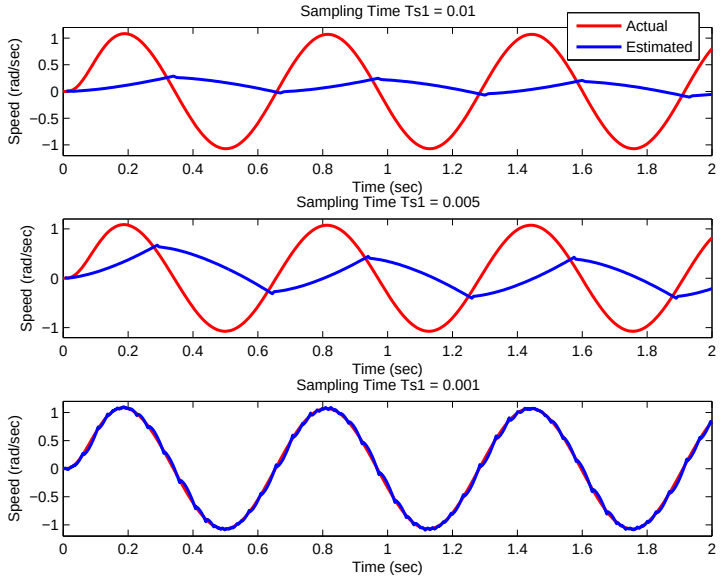

Figure 30: *Effects of sampling rates: sinusoid response*

5.3.3 Impact on Noise Attenuation

Signal measurements and communications introduce noises. One of the feedback functions is to attenuate noises so that the motor speed fluctuation can be reduced. In the previous case studies, we have already see that noise attenuation is a factor to be considered. To demonstrate more concretely this aspect of design considerations, we choose three cases of small, medium, and large noises in the following example.

Example 11 Consider the same PMDC specifications as in Example 8 with fixed weight $\alpha_1 = 0.98$ and sampling interval $T_{s1} = 0.01$ sec. We add noises to the output communication block with mean zero and standard deviation σ. Then the signal estimator (5.19) is applied for three cases of noise variances. Figure 31, Figure 32, and Figure 33 illustrate control performance under different input commands.

Discussions: From Figures 31, 32, and 33, large noises must be attenuated. Noise attenuation capability depends on selections of α_1 and T_{s1}. In the case of small noises, the top plots of the figures, noise attenuation is not a big concern. But as noise variances increase, the motor performance is no longer acceptable. In these cases, α_1 and T_{s1} must be re-designed so that noise attenuation ability is balanced with other performance measures.

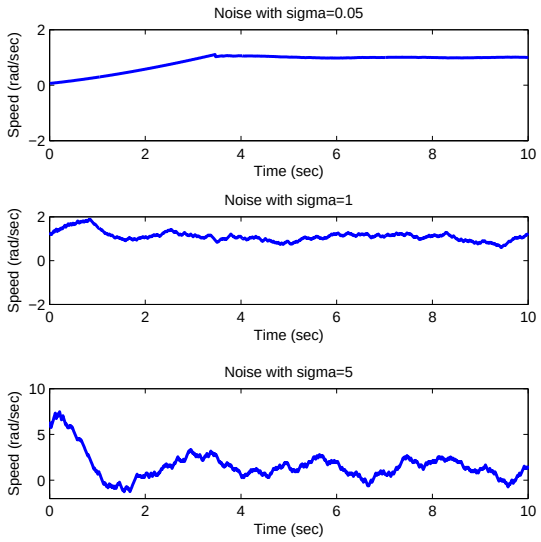

Figure 31: *Effects of noise: step response*

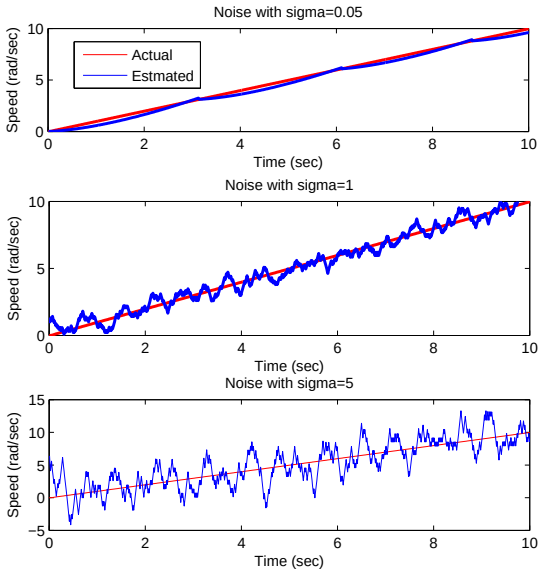

Figure 32: *Effects of sampling rates: ramp response*

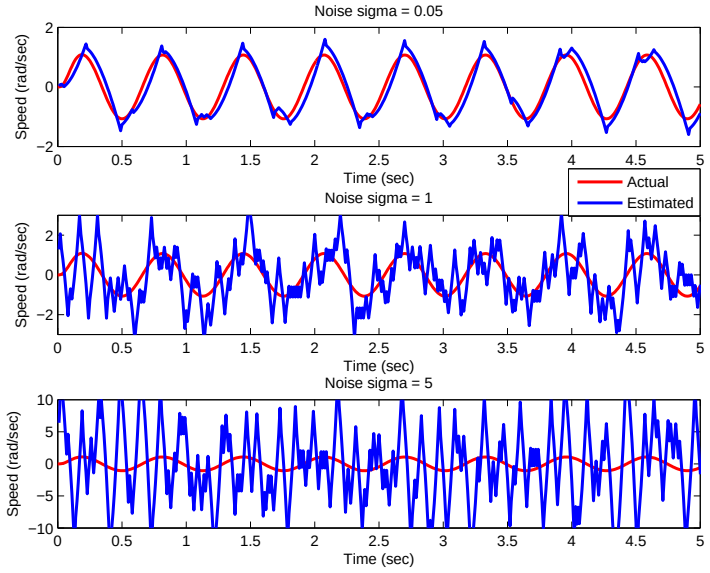

Figure 33: *Effects of sampling rates: sinusoid response*

5.4 Case Study 2: Both Input and Output Communication Blocks

This section will consider more realistic cases of two communication blocks, shown in Figure 23. Analysis of such systems can be carried out using the same methods as in Section 5.2. We will use some typical scenarios to demonstration design variables and their impact, and provide some guidelines.

5.4.1 Impact of Signal Averaging Weights α_1 and α_2

We first consider the impacts of signal averaging weights α_1 and α_2 on the performance of the PMDC system using both communication blocks 1 and 2.

Example 12 Consider the same PMDC specifications as in Example 8. In this example the sampling intervals for both communication blocks are $T_{s1} = T_{s2} = 0.001$ sec, Then the signal estimator (5.19) is applied. Three cases are considered with $\alpha_1 = \alpha_2 = \alpha$. Figure 34 shows the step response of the closed-loop system with performance parameters summarized in Table 9. Figures 35 and 36 expand performance evaluation to the ramp and sinusoid inputs.

Discussions: From Figure 34 and Table 9 we can see that the signal averaging weights α_1 and α_2 have similar influence on the system as in the one-block case: as α_1 and α_2 are increased, the rise time, settling time, and peak time will increase. On the other hand, the overshoot becomes smaller. This trade-off can be explained by the data window sizes. Larger weights entail larger data windows, which in turn imply

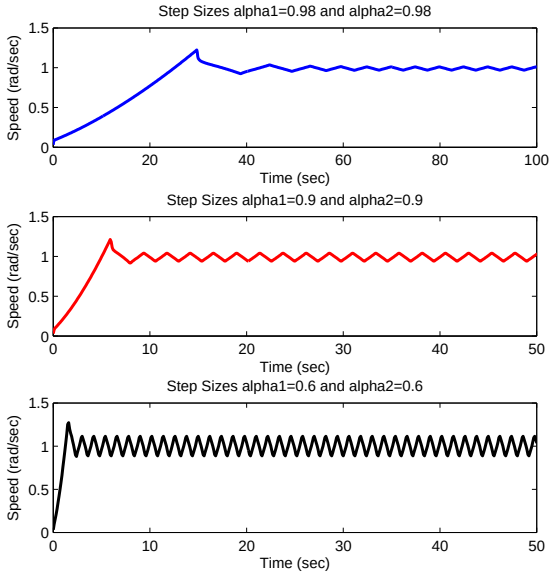

Figure 34: *Effect of signal averaging weights: step response*

slower dynamics from the filters. Consequently, the closed-loop system demonstrates typical changes in its performance associated with slow dynamics. Slow systems compromise tracking capability, shown in Figures 35 and 36. The main implication is that if tracking performance (such as acceleration) is essential, then small α values should be used.

Table 9: Step Response Performance of Figure 34

$\alpha_1 = \alpha_2$	t_r	t_s	t_{max}	M_p
0.98	22.4	32.2	29.8	22.28
0.90	4.6	7.2	6.0	21.23
0.60	1.1	4.5	1.7	27.19

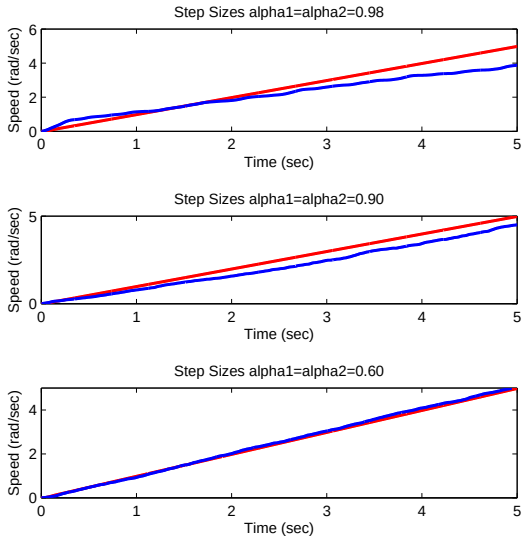

Figure 35: *Effect of signal averaging weights: ramp response*

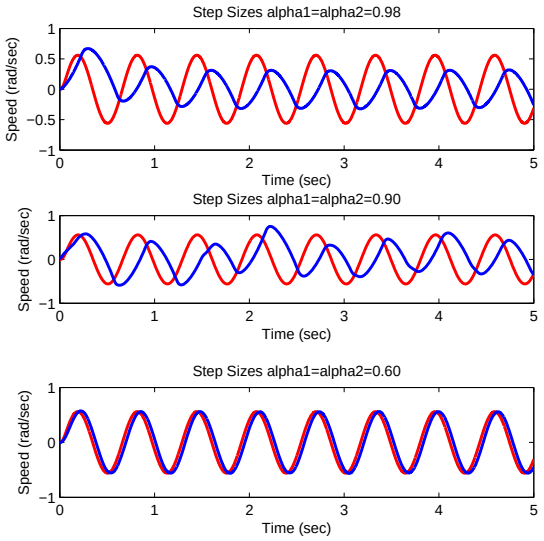

Figure 36: *Effect of signal averaging weights: sinusoid response*

Example 13 Consider the same PMDC specifications and sampling rates as in Example 8. Then the signal estimator (5.19) is applied for 3 cases such that unequal values of α's for both blocks ($\alpha_1 \neq \alpha_2$). Figure 37 and Table 10shows the output speed response of closed loop PMDC motor and the performance measure.

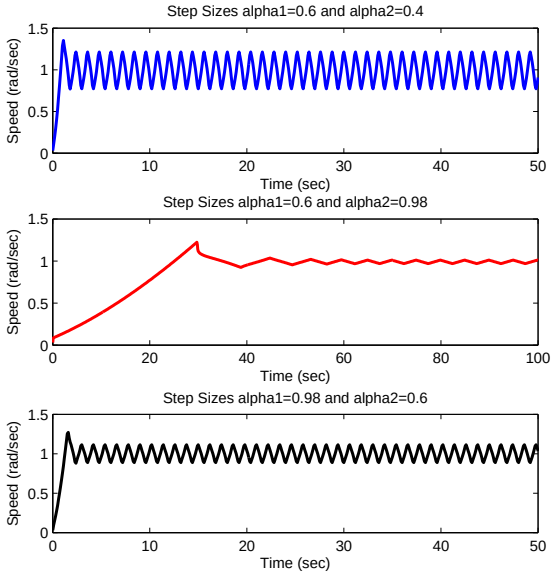

Figure 37: *Effects of different signal averaging on closed loop using two blocks*

Table 10: Step Response Performance of Figure 37

α_1, α_2	t_r	t_s	t_{max}	M_p
0.60,0.40	1.2	NA	1.6	37.8
0.60,0.98	22.6	32.5	30.21	24.28
0.98,0.60	1.2	5.2	1.8	27.19

5.4.2 Impact of Sampling Intervals T_{s1} and T_{s2}

Example 14 Consider the same PMDC specifications as in Example 8 with fixed $\alpha_1 = \alpha_2 = 0.60$. Then the signal estimator (5.19) is applied. The sampling intervals $T_{s1} = T_{s2}$ are varied to assess their impacts on feedback performance. Figure 38 shows the step response with supporting details in Table 11. Similarly, Figure 39 is for the ramp input, and Figure 40 is for the sinusoid input.

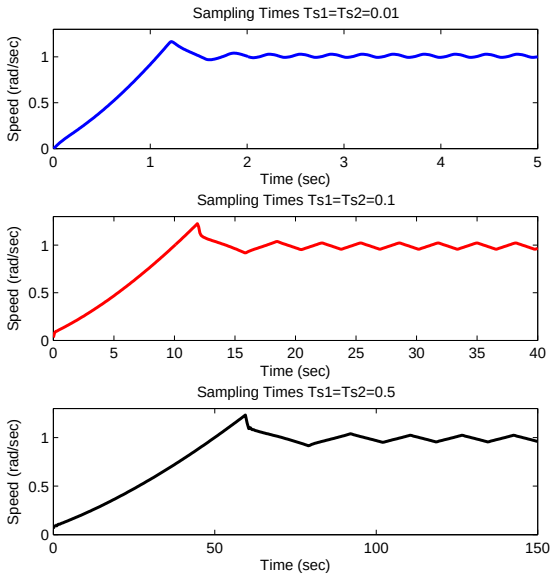

Figure 38: *Effects of sampling intervals: step response*

Discussions: From Figure 38 and Table 11, as T_{s1},T_{s2} increase, the rise time, settling time, and the peak time increase, while the overshoot is reduced.

From Figures 36 and 40, it is cleared that to retain desirable performance, α_1 and α_2 should be adapted according to T_{s1},T_{s2}. This will avoid loss of robustness of the feedback system when communication data flow rates fluctuate from communication

traffic conditions.

Furthermore, two blocks of dynamic subsystems alter the loop dynamics significantly. It may make it necessary to re-design the controller itself. In our studies, the following adaptation strategies are used to make controller parameter K_c dependent on the sampling interval. The typical values are: when $T_{s1} = T_{s2} = 0.01$, $K_c = 20.8$; when $T_{s1} = T_{s2} = 0.1$, $K_c = \frac{1}{1.8}$; when $T_{s1} = T_{s2} = 0.5$, $K_c = \frac{1}{10.7}$. The principle is that for slow sampling (large sampling intervals), the controller should be make more conservative.

Table 11: Step Response Performance of Figure 38

$T_{s1} = T_{s2}$	t_r	t_s	t_{max}	M_p
0.01	0.88	3.86	1.23	16.67
0.10	8.9	30.1	12.0	22.5
0.50	45.0	120.4	60.0	23.26

Example 15 Consider the same PMDC specifications as in Example 8 with fixed step sizes $\alpha_1 = \alpha_2 = 0.95$. Then the signal estimator (5.19) is applied for 3 cases such that unequal values of sampling rates for both blocks $T_{s1} \neq T_{s2}$. Figure 41 and Table 12 show the output speed response of closed loop PMDC motor and performance measure.

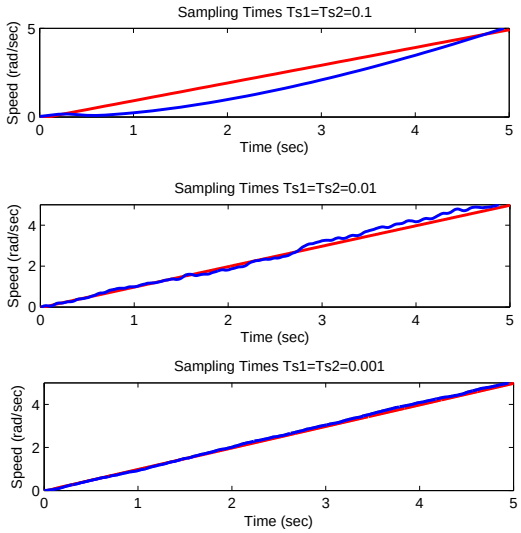

Figure 39: *Effects of sampling rates: ramp response*

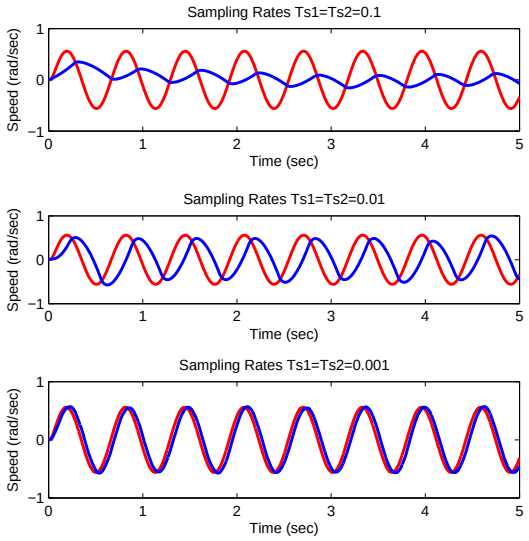

Figure 40: *Effects of sampling rates: sinusoid response*

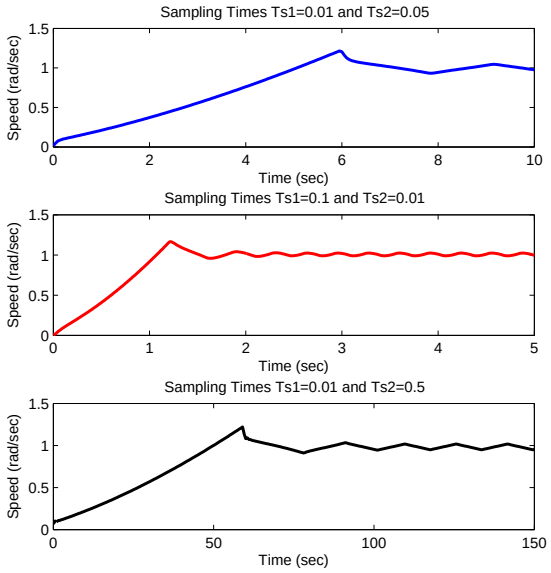

Figure 41: *Effects of different sampling rates on closed loop using two blocks*

Table 12: Step Response Performance of Figure 41

T_{s1}, T_{s2}	t_r	t_s	t_{max}	M_p
0.01,0.05	4.88	9.94	5.87	18.87
0.10,0.01	0.83	3.1	1.27	21.5
0.01,0.50	47.0	125.4	61.0	24.26

5.4.3 Impact of Transmission Errors and Packet Losses

The channel Υ is characterized by the probability transition matrix

$$\Pi = \begin{bmatrix} \pi_{11} & \pi_{12} & \pi_{13} \\ \pi_{21} & \pi_{22} & \pi_{23} \end{bmatrix}$$

with $\sum_{j=1}^{3} \pi_{ij} = 1$, $i = 1, 2$. Here,

$$\pi_{11} = P\{x_k = 0 | s_k = 0\},\ \pi_{12} = P\{x_k = 1 | s_k = 0\},\ \pi_{13} = P\{x_k = * | s_k = 0\}$$

$$\pi_{21} = P\{x_k = 0 | s_k = 1\},\ \pi_{22} = P\{x_k = 1 | s_k = 1\},\ \pi_{23} = P\{x_k = * | s_k = 1\}.$$

Let $p = P\{x_k = 0 | s_k = 0\} = P\{x_k = 1 | s_k = 1\}$, $q = P\{x_k = * | s = 0\} = P\{x_k = * | s = 1\}$, $p^s = P\{s_k = 1\}$, $p^x = P\{x_k = 1\}$. For a symmetric channel, we have $\pi_{13} = \pi_{23}$ (the probability of data loss) and $\pi_{11} = \pi_{22}$ (the probability of correct data transmission). Then

$$\Pi = \begin{bmatrix} p & 1-p-q & q \\ 1-p-q & p & q \end{bmatrix} \tag{5.34}$$

Assumption 2 $2p + q - 1 \neq 0$.

The case $2p+q-1 = 0$ means that $p = (1-q)/2$. This implies that if the data are not lost (which has probability $1-q$), then the channel output has an equal probability of receiving 1 or 0 regardless what is the input symbol. This is the singular case and the channel does not transmit any information, as evidenced in Shannon's information theory. Since $p^x = pp^s + (1-p-q)(1-p^s) = (2p+q-1)p^s + 1 - p - q$, under Assumption 2, p^s can be calculated from p^x

$$p^s = \frac{p^x - (1-p-q)}{(2p+q-1)}. \tag{5.35}$$

In addition, communication channels introduce time delays. Suppose that a time delay of τ seconds is in effect in data transmission at a given time. Under the sampling interval T_s, this time delay is translated into $n_d = \tau/T_s$ steps of delay in discrete time. For notational simplicity, assume that n_d is an integer. Note that for any given τ, $n_d \to \infty$ when $T_s \to 0$. In other words, for a meaningful discussion of effect of time delay on systems in asymptotic analysis, n_d must be varied so that $n_d T_s = \tau$ is a constant.

In many practical systems with communication channels, it is desirable to reduce communication power and bandwidth consumption, and perform signal processing at the receiving side. We shall consider the case of the binary scheme for quantization and DMC communication channels. Let $w_k = H(s_k)$ represent the channel.

Signal estimation and feedback control algorithms are modified to be:

$$\begin{aligned}
x_{k+1} &= x_k + T_s(Ax_k + Bu_k) \\
\omega_k &= Cx_k \\
s_k &= \begin{cases} 1, & \omega_k + d_k \le h \\ 0, & \omega_k + d_k > h \end{cases} \\
w_k &= H(s_k) \\
\widetilde{\xi}_{k+1} &= \widetilde{\xi}_k + \beta(w_k - \widetilde{\xi}_k) \\
\xi_k &= \frac{\widetilde{\xi}_k - (1-p-q)}{(2p+q-1)} \\
\widehat{\omega}_k &= h - F^{-1}(\xi_k) \\
u_k &= -\widehat{\omega}_k.
\end{aligned} \tag{5.36}$$

Remark 5 In this algorithm, the channel information p and q are assumed to be known. Joint identification of the signal ω_k and the channel parameters p and q can be derived directly from the joint identification algorithms in [41]. This will not be included here.

Definition 1 *ω_k is slowly varying if $|\omega_k - \omega_{k-1}| \leq r$ for some small r.*

By [43], we have the following result.

Lemma 3 *if α is selected as a function of r such that $1-\alpha(r) \to 0$ and $\sqrt{r}/(1-\alpha(r)) \to 0$ as $r \to 0$, the algorithm (5.18) has the following property:*

$$\lim_{r\to 0} \frac{1+\alpha(r)}{1-\alpha(r)} E(\widehat{y}_k - \omega_k)^2 = \frac{F(h-\omega_k)(1-F(h-\omega_k))}{f^2(h-\omega_k)}.$$

Theorem 8 *The asymptotic signal estimation error is*

$$\lim_{\alpha\to 1} \frac{1+\alpha}{1-\alpha} E(\widehat{\omega}_k - \omega_k)^2 = \frac{(aF(h-\omega_k)+b)(1-(aF(h-\omega_k)+b))}{a^2 f^2(h-\omega_k)}, \tag{5.37}$$

where $a = 2p+q-1$ and $b = 1-p-q$.

Proof: (5.37) follows from Lemma 3 with

$$\begin{aligned}
\lim_{\alpha\to 1} \frac{1+\alpha}{1-\alpha} E(\widehat{\omega}_k - \omega_k)^2 &= \frac{p^x(1-p^x)}{(dp^x/d\omega_k)^2} \\
&= \frac{(ap^s+b)(1-(ap^s+b))}{a^2(dp^s/d\omega_k)^2} \\
&= \frac{(aF(h-\omega_k)+b)(1-(aF(h-\omega_k)+b))}{a^2 f^2(h-\omega_k)}.
\end{aligned}$$

□

By Theorem 8, we have the following system representation.

Corollary 1 *when* $\alpha \to 1$ $H(z) = \frac{(1-\alpha)z}{z-\alpha}$ *and* $\{d_k\}$ *is a sequence of i.i.d. random variables satisfying* $Ed_k = 0$ *and* $Ed_k^2 = \frac{(aF(h-\omega_k)+b)(1-(aF(h-\omega_k)+b))}{a^2 f^2(h-\omega_k)}$.

Remark 6 We point out that communication errors and packet losses increase the variance of the equivalent noise, but do not alter the structure of the closed-loop system. Consequently, under Assumption 2, the stability analysis and performance tradeoff presented in the previous sections remain valid here.

5.4.4 Impact of Communication Delays

Communication channels always encounter time delays. Communication latency indicates that the data point s_k sent at time t_k will arrive at the receiver buffer at $t_k^r = t_k + \widetilde{\tau}_k$. Assuming that the channel hubs employ FIFO (first-in-first-out) buffers, the data sequence will not be altered despite time-varying delays $\widetilde{\tau}_k$. Suppose that the sampling of s_k is synchronized with $t_k = kT_s$ where T_s is the sampling interval. Then w_k is received at $t_k^r = \max\{t_k + \widetilde{\tau}_k, t_{k-1}^r\}$. In other words, if s_k is subject to a much shorter delay than s_{k-1}, it will be considered as received immediately after w_{k-1} is received.

Suppose the channel is subject to a constant but unknown time delay τ. For simplicity, we focus on time delay and assume that the channel has no other uncertainty. For a small sampling interval T_s, the overall closed-loop system with signal estimation on ω becomes

$$\begin{aligned}
x_{k+1} &= x_k + T_s(Ax_k + Bu_k) && \text{(plant)} \\
\omega_k &= Cx_k \\
s_k &= \begin{cases} 1, & \omega_k + d_k \le \gamma \\ 0, & \omega_k + d_k > \gamma \end{cases} && \text{(quantization)} \\
w_k &= s_{k-\tau/\beta} && \text{(channel delay)} \\
\xi_{k+1} &= \xi_k + \beta(w_k - \xi_k) && \text{(signal averaging)} \\
\widehat{\omega}_k &= \gamma - F^{-1}(\xi_k) && \text{(signal exponential estimation)} \\
u_k &= -\widehat{\omega}_k. && \text{(feedback)}
\end{aligned} \tag{5.38}$$

Chapter 6: CONCLUSION AND FUTURE WORK

6.1 Conclusion

This dissertation introduces a new method of identifying the model parameters and predicts the rotational speed of PMDC motors, using quantized output observations. This technique is useful in reducing costs of motor sensing systems, communication resource consumptions, and in enhancing system reliability by simplifying system configuration and packaging. While the PMDC motor is used as a benchmark case for discussion, it appears that the same method can be applied to other electric machines.

The binary identification technology was explored for nonlinear systems in [70]. In particular, Wiener and Hammerstein systems can be accommodated. This may be valuable for PMDC motors when we take further consideration of their nonlinear components. Although, we have applied our methodology to PMDC motors, it can be applied to other electric machines as well. The adaptation of proposed system gives the system the ability to use in on-line identification and real time estimation.

In this dissertation, the impact of communication channels on feedback performance of PMDC motors is also studied. The main conclusions of this study indicate that when communications and signal estimations are involved, sampling intervals and signal averaging window sizes (or equivalently signal estimation step size) must be carefully coordinated so that performance specifications can be robustly maintained. The situations are further complicated by the noise attenuation capability

and tracking performance of the system which are also substantially affected by the same design parameters. The results of this dissertation show that there is a basic relationship between the sampling interval and signal averaging weight that can be used to adapt the weight when communication data flow rates change with time. Finally, as part of the feedback loop, the controller itself may need to be re-designed to accommodate communication channels.

6.2 Future Work

Along these directions, there are some remaining work that need to be completed in the near future. In this section 6.2, several topics are suggested to supplement the current work as the future research efforts.

1. Hardware embedded system implementation of real time estimation system: In order to build the hardware system the following components should be available:

    - PMDC Motor
    - Binary Speed Sensor (Hall Effect sensor WGB351928 or IR Infrared sensor LM393)
    - DC Power Supply Voltage up to 120 volts.
    - Microcontroller PIC18F2455 or PIC16F877A (Any PIC Microcontroller with PWM output)

- RS232 Serial Communication port (to transmit the output pulses of the speed to PC)
- PMDC Motor Driving Circuit (Dual full bridge chip L298 or Non Inverting Buck Boost driving chip or H bridge chip with suitable voltage applicable to our PMDC motor)

Procedures

(a) Using MPLAB IDE software and C code to program the PIC Microcontroller to give us a PWM signal with variable Duty Cycle; this can be done using two timers built in microcontroller.

(b) Build the Driving circuit using switching techniques (Dual full bridge chip L298 or Non Inverting Buck Boost driving chip or H bridge chip with suitable voltage applicable to our PMDC motor), then using the variable PWM to control the input average DC voltage applied to the motor in periodic form (our case is 4-periodic).

(c) After that the output speed is measured for each input value using binary speed sensor.

(d) Using the RS232 interface, the binary output of the sensor is transmitted to the PC computer.Figure 42 shows the hardware diagram of the system.

(e) Using the Lab View software 2011, the real time data is processing online

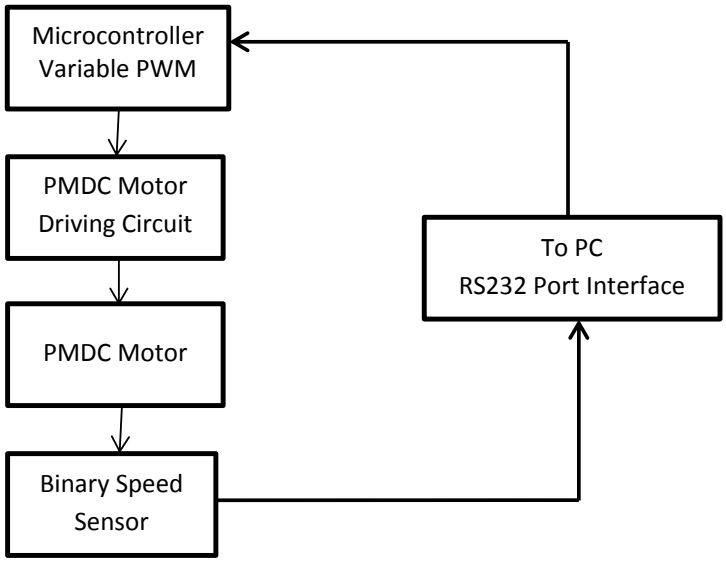

Figure 42: *Hardware implementation of real time estimation of PMDC parameters*

to estimate the parameters of the PMDC motor. The estimation process can be done simultaneously for any number of observations N during the time measured. Note: At each interruption (each 0.39321s), the value of speed counter, will be taken as detected pulses. The pulses produced from binary speed sensor for each speed, will be loaded to PC each 0.39321s. So, the motor speed is calculated using some equations.

2. Hardware implementation of closed loop feedback system with communication channels:

   This system can be implemented wireless also by transmitting the speed signal through a wireless communication channel, then do the controller part and re-submit the controller signal to the PMDC motor again.

Procedure

Using the same component in the first part, then the output speed signal can be transmitted/recieved using Zigbee wireless software.

3. Detection of fault Diagnosis for PMDC motors In PMDC motors faults can occur in the rotor/field, stator/armature, or mechanical components connected to it. This dissertation discusses a permanent magnet machine without focusing on associated inverter faults and bearing faults.

   Types of Faults:

   - Armature faults

     The armeture faults are usually happened when the winding insulation failure, this is because of manufacturing defect, high operation temperature, overloading, vibration, or transient high voltage. This fault may start from a short circuit between two turns, or phase to ground short.

   - Permanent Magnetic Faults

     Field faults basically refers to a failure in the permanent magnets, this cause the demagnetization to be uniform over all poles or partial over certain region or poles, this fault can be caused by high operation temperature, aging of magnets, corrosion of magnets, or inappropriate armature current.

   - Mechanical Faults

Mechanical faults can happen because of bearing failure. A bearing is a mechanical component which consists of two rings and a set of balls rolling between them. This has been recorded as one of the dominant causes for damage in electric machine, this fault can be caused by metal fatigue, unbalanced stress, improper installation, corrosion.

These problems could result in vibrations and noise during the machine's operation, which are usually measured and processed as diagnosis indicators.

It is clear that motor parameters will be changed according to motor faults therefore, it is easy to detect a motor fault by comparing its estimated parameters with normal parameters. When parameter change exceeds a preset threshold, a fault is immediately detected, because the pattern of parameter changes is different for different faults. Sometimes one fault causes different parameters to be changed; in this case it is difficult to detect the fault.

4. Impact of transmission errors and packet losses:

   In many practical systems with communication channels, it is desirable to reduce communication power and bandwidth consumption, and perform signal processing at the receiving side. So, some simulation can be done to study the impact of transmission errors and packet losses.

5. Impact of communication delays:

   Communication channels always encounter time delays. In this case also some simulation results can be done to study the impact of communication delays on

the response of the system.

6. Designing the graphical user interface (GUI) of the proposed system that can be developed using LabView or MatLab software, this technology can be easily handled, so it can be available for most of the people without complicated. Also this design can be applied to the front panel of any type of vehicles.

REFERENCES

[1] A.K. Rao, Y. F. Huang, S. Dasgupta, "ARMA parameter estimation using a novel recursive estimation algorithm with selective updating," Acoustics, Speech and Signal Processing, IEEE Transactions on , vol.38, no.3, pp.447-457, Mar 1990.

[2] A.J. Blauch, M. Bodson, J. Chiasson, "High-speed parameter estimation of stepper motors," Control Systems Technology, IEEE Transactions on , vol.1, no.4, pp.270-279, Dec 1993.

[3] K. Kyeong-Hwa, S. Chung; G. Moon; I. Baik; M. Youn, "Parameter estimation and control for permanent magnet synchronous motor drive using model reference adaptive technique,"Industrial Electronics, Control, and Instrumentation, 1995.,

[4] D.C. Huynh, "On-line parameter estimation o f an induction machine using a recurcive least squares algoritiun with multiple time-varying forgetting factors, "presented at 2010Power and Energy(pECon).Conf.

[5] S. M. Kay, Fundamentals of Statistical Signal Processing: Estimation Theory. Englewood Cliffs, NJ: Prentice-Hall, 1993.

[6] M. Samonas and M. Petrou, "A peak preserving algorithm for the removal of colored noised from signals," IEEE Trans. Signal Process., vol. 50, no. 11, pp. 2683-2693, Nov. 2002.

[7] L. Ljung System identification: Theory for the user Prentice-Hall, Englewood Cliffs, NJ (1987).

[8] S. Billings, Identification of nonlinear systems-a survey, Proc. IEE-D, 127 (1980), pp. 272- 285.

[9] B. Ninness and S. Gibson, Quantifying the accuracy of Hammerstein model estimation, Automatica J. IFAC, 38 (2002), pp. 2037-2051.

[10] A. Isik, O. Karakaya, P.A. Oner, M.K. Eker , "PMDC motor speed control with fuzzy logic algorithm using PIC16F877 micro controller and plotting data on monitor," Soft Computing, Computing with Words and Perceptions in System Analysis, Decision and Control, 2009. ICSCCW 2009.

[11] C. Laughman, S.B. Leeb, L.K Norford, S.R. Shaw, P.R Armstrong, "A two-step method for estimating the parameters of induction machine models," Energy Conversion Congress and Exposition, 2009. ECCE 2009. IEEE , vol., no., pp.262-269, 20-24 Sept. 2009.

[12] S. Udomsuk, K.L. Areerak, K.N. Areerak, A. Srikaew, "Parameters identification of separately excited DC motor using adaptive tabu search technique," Advances in Energy Engineering (ICAEE), 2010 International Conference on , vol., no., pp.48-51, 19-20 June 2010.

[13] M.F. Moussa, M. Saad, Y.G. Dessouky, "Adaptive control and one-line identification of sensorless permanent magnet DC motor," Computational Technologies

in Electrical and Electronics Engineering(SIBIRCON), 2010 IEEE , vol., no., pp.852-857, 11-15 July 2010.

[14] V. I. Utkin, "Sliding mode control design principles and applications to electric drives," Industrial Electronics, IEEE Transactions on , vol.40, no.1, pp.23-36, Feb 1993.

[15] V. I. Utkin, H. Chang, "sliding mode control on electro-mechanical systems", Mathematical Problems In Engineering, 2002, Taylor and Francis Group.

[16] A.M. Sharaf, E. Elbakush, and I.H. Altas, "A Predictive Dynamic Controller for PMDC Motor Driver", The 5th International Conference on Industrial Automation, Ecole de Technologie Superieure (Universite du Quebec), Montreal, Canada June 11-13, 2007.

[17] A.Pisano, A. Davila, L. Fridman, E. Usai, "Cascade Control of PM DC Drives Via Second-Order Sliding-Mode Technique," Industrial Electronics, IEEE Transactions on , vol.55, no.11, pp.3846-3854, Nov. 2008.

[18] Sang-Hoon Chu; In-Joong Ha; Sung-Joon Lee; Joon-Hyuk Kang, "Feedback-linearizing control of hybrid step motors," Industrial Electronics, Control and Instrumentation, 1994. IECON '94., 20th International Conference on , vol.3, no., pp.2039,2044 vol.3, 5-9 Sep 1994.

[19] Maamri, N.; Gaubert, J-P; Trigeassou, J. C.; Moreau, S., "Speed Controller Using Time Constrained Output Feedback for Permanent Magnet DC Motor,"

Industrial Electronics, 2007. ISIE 2007. IEEE International Symposium on , vol., no., pp.1153,1158, 4-7 June 2007.

[20] Ivo Petr s "FRACTIONAL - ORDER FEEDBACK CONTROL OF A DC MOTOR" Journal of ELECTRICAL ENGINEERING, VOL. 60, NO. 3, 2009, 117-128.

[21] Fisher, M.E.; Ghosh, A.; Sharaf, A.M., "Intelligent control strategies for permanent magnet DC motor drives," Power Electronics, Drives and Energy Systems for Industrial Growth, 1996., Proceedings of the 1996 International Conference on , vol.1, no., pp.360,366 vol.1, 8-11 Jan 1996.

[22] Weiyao Lan; Qi Zhou, "Speed control of DC motor using composite nonlinear feedback control," Control and Automation, 2009. ICCA 2009. IEEE International Conference on , vol., no., pp.2160,2164, 9-11 Dec. 2009.

[23] Saurav, Kumar; Potluri, Ramprasad, "Sensorless speed control of a permanent magnet DC motor by compensating the plant nonlinearities," Industrial Electronics (ISIE), 2013 IEEE International Symposium on , vol., no., pp.1,4, 28-31 May 2013.

[24] Wisnu Djatmiko, and Bambang Sutopo, "Speed Control DC Motor under Varying LoadUsing Phase-Locked Loop System". Proc. of the International Conf. on Electrical, Electronics, Communication, and Information CECI'2001, March 7-8, Jakarta.

[25] T. Wigren, Convergence analysis of recursive identification algorithms based on the nonlinear Wiener model, *IEEE Transactions on Automatic Control*, Volume 39, Issue 11, pp. 2191 - 2206, 1994.

[26] J. Voros, Parameter identification of Wiener systems with multisegment piecewise-linear nonlinearities, *Systems and Control Letters*, Volume 56, Issue 2, pp. 99 - 105, 2007.

[27] E. W. Bai, An optimal two-stage identification algorithm for Hammerstein-Wiener nonlinear system, *Automatica*, vol. 34(3), pp. 333-338, 1998.

[28] H. F. Chen, Recursive identification for Wiener model with discontinuous piecewise linear function, *IEEE Trans. Autom. Control*, vol. 51(3), pp. 390-400, 2006.

[29] Y. Zhao, L.Y. Wang, G. Yin, J.-F. Zhang, Identification of Wiener systems with binary-valued output observations, *Automatica*, **43**, pp. 1752-1765, 2007.

[30] P. Bolzern, P. Colaneri, and G.De Nicolao, Finite escapes and convergence of robust H^2 filters, *Automatica*, Vol.33, N.1, pp. 31-47, 1997.

[31] P. Colaneri, A. Ferrante, Algebraic Riccati equation and J-spectral factorization in H^∞ estimation, *Systems and Control Letters*, Vol. 51, pp. 383-393, 2004.

[32] P.R. Khargonekar, M.A. Rotea, and E. Baeyens, Mixed H^2/H^∞ filtering, *Int. J. Robust Nonlinear Control*. v6 i6. 313-330, 1996.

[33] C.E. de Souza, R.M., Palhares, and P.L.D. Peres, Robust H^{∞} filtering design for uncertain linear systems with multiple time-varying state delays, *IEEE Trans. Signal Processing*, Vol. 49, Issue 3, pp. 569-576, 2001.

[34] J.S. Freudenberg, R.H. Middleton, V. Solo, Stabilization and Disturbance Attenuation Over a Gaussian Communication Channel, *IEEE Trans. Autom. Control*, vol. 55, pp. 795-799, 2010.

[35] G.N. Nair, F. Fagnani, S. Zampieri, and R.J. Evans, Feedback control under data rate constraints: An overview, *Proc. IEEE*, vol. 95, no. 1, pp. 108-137, Jan. 2007.

[36] A. S. Y k sel and T. Basar, Optimal signaling policies for decentralized multicontroller stabilizability over communication channels, *IEEE Trans. Autom. Control*, vol. 52, no. 10, pp. 1969-1974, Oct. 2007.

[37] N. C. Martins and M. A. Dahleh, Feedback control in the presence of noisy channels: Bode-like fundamental limitations of performance, *IEEE Trans. Autom. Control*, vol. 53, no. 7, pp. 1604-1615, Aug. 2008.

[38] A.S. Matveev and A.V. Savkin, The problem of LQG optimal control via a limited capacity communication channel, *Syst. Control Lett.*, vol. 53, no. 1, pp. 51-64, 2004.

[39] A. J. Rojas, J. H. Braslavsky, and R. H. Middleton, Fundamental Limitations in Control over a Communication Channel *Automatica*, vol. 44, pp. 3147-3151, 2008.

[40] M. Casini, A. Garulli and A. Vicino, "Time complexity and input design in worst-case identification using binary sensors", *Proceedings of the* 46$^{\text{th}}$ *IEEE Conference on Decision and Control*, pp. 5528-5533, New Orleans, LA, USA, Dec. 12-14, 2007.

[41] L.Y. Wang, G. Yin, J.-F. Zhang, and Y.L. Zhao, *System Identification with Quantized Observations*, Birkhäuser, Boston, MA,

[42] Le Yi Wang, George Yin, Chanying Li, Wei Xing Zheng, Feedback systems with communications: Integrated study of signal estimation, sampling, quantization, and feedback robustness, International Journal of Adaptive Control and Signal Processing, accepted and to appear in 2013.

[43] L.Y. Wang, G. Yin, C.Y. Li, W.X. Zheng, Signal estimation with binary-valued sensors, *Journal of Systems Science and Complexity*, vol. 23, pp. 622-639, 2010.

[44] A. Benveniste, M. Metivier, and P. Priouret, *Adaptive Algorithms and Stochastic Approximations*, Springer-Verlag, Berlin, 1990.

[45] H.-F. Chen and L. Guo, *Identification and Stochastic Adaptive Control*, Birkhäuser, Boston, MA, 1991.

[46] H. J. Kushner and G. Yin, *Stochastic Approximation and Recursive Algorithms and Applications*, 2nd Ed., Springer-Verlag, New York, 2003.

[47] P. Billingsley, *Convergence of Probability Measures*, Wiley, New York, NY, 1968.

[48] Y.S. Chow and H. Teicher, *Probability Theory*, 3rd Ed., Springer-Verlag, New York, 1997.

[49] R. Z. Khasminskii, *Stochastic Stability of Differential Equations*, Sijthoff and Noordhoff, Alphen aan den Rijn, Netherlands, 1980.

[50] J. Chiasson, Modeling and High-Performance Control of Electric Machines, John Willey & Sons, 2005.

[51] James Larminie and John Lowry, Electric Vehicle Technology Explained, 2nd Edition, John Wiley & Sons, 2012.

[52] Chris Mi, Abul Masrur, David Gao, Hybrid Electric Vehicles: Principles and Applications with Practical Perspectives, John Wiley & Sons, 2011.

[53] Robert Bosch GmbH, Bosch Automotive Handbook, 8th Edition, John Wiley & Sons, 2011.

[54] A.M. Sharaf, E. Elbakush, and I.H. Atlas, A Predective Dynamic Controller For PMDC Motor Drives. The fifth International Conference on Industrial Automation, Montreal, Quebec, Canada, June 11-13, 2007.

[55] J. R.Cogdell "Foundations of Electrical Engineering", Prentice Hall, Englewood Cliffs, NJ, 1990.

[56] H. A. Nielsen, H. Madsen, "Predicting the Heat Consumption in District Heating Systems using Meteorological Forecasts", Department of Mathematical Modelling, Technical University of Denmark 2000.

[57] H. A. Nielsen, H. Madsen, "Modelling the heat consumption in district heating systems using a grey-box approach", Energy and Buildings,38 (1), 63-71,doi:10.1016/j.enbuild.2005.05.002 (2006)

[58] A. C. Schouten, E. Vlugt and F. C. T. van der Helm "System Identification And Parameter Estimation" Version: March 8, 2007.

[59] D. J. Murray-Smith, Methods of system identification, parameter estimation and optimization applied to problems of modeling and control in engineering and physiology. DSc thesis, University of Glasgow. 2009

[60] T. Soderstom and P. Stoica, System Identification, Printice Hall, 1989.

[61] K. Ogata, *Morden Control Engineering*, 4th Edition, Prentice-Hall, Englewood Cliffs, NJ, 2002.

[62] Bhag S. Guru and Huseying R. Hiziroglu, Electric Machinary And Transformers, Oxford University Press, 2001.

[63] Vadim I. Utkin and Hao-Chi Chang, Sliding Mode Control on Electromechanical Systems, Mathmetical Problems in Engineering, Vol, pp, 451-473, 2002.

[64] Craiu, O., A. Machedon, et al. (2010). 3D Finite Element thermal analysis of a small power PM DC motor. 12th International Conference on Optimization of Electrical and Electronic Equipment (OPTIM), 2010.

[65] A.E. Fitzgerald, Charles Kingsley Jr., and Stephen D. Umans, Electric Machinery, McGraw-Hill Science/Engineering/Math; 6th edition (July 25, 2002).

[66] D. Hanselman, "Brushless Permanent Magnet Motor Design", 2nd Edition, The Writers' Collective, Cranston, Rhode Island, 2003.

[67] J. Anthony "Pansini Electrical Distribution Engineering", Third Edition, (Nov 10, 2006).

[68] L. Y. Wang, J. F. Zhang, and G. Yin, System identification using binary sensors, IEEE Transactions on Automatic Control, 48, 1892-1907.

[69] L. Y. Wang, G. Yin, and J. F. Zhang, Joint identification of plant rational models and noise distribution functions using binary-valued observations, Automatica, 42, 533-547, 2006.

[70] L. Y. Wang, G. Yin, and Y.L. Zhao, System identification with quantized observations, Birkhauser, Boston, 2010.

[71] Dorf, R.C, and Bishop, R.H., 2010, "Modern Control Systems", 12th edition, USA, Prentice Hall.

[72] Franklin, G.F., Powell, J.D, and Emami-Naeini, A., 2010, "Feedback Control of Dynamic Systems", 6th edition, USA, Pearson.

[73] L. Y. Wang and G. Yin, Asymptotically efficient parameter estimation using quantized output observations,Automatica, 43, 1178-1191, 2007.

[74] K. Ogata, "System Dynamics", 4nd Edition, Prentice Hall, Englewood Cliffs, New Jersey, NJ, 1996.

[75] Cherry Electrical Products, "Comparing Speed Sensor Technologies" Hall and VR" , This article was posted on 10/01/2000.

[76] http://www.infolytica.com, http://www2.electronicproducts.com

[77] G. Hysteresis in Magnetism: For Physicists, Materials Scientists, and Engineers, San Diego: Academic Press, 1998

[78] A. E. Fitzgerdal, C. Jr. Kingsley, S. D. Umans, (Electric Machinery (4th ed.) Mc-Graw-Hill, Inc.. pp. 20. 1983 ISBN 0-07-021145-0

[79] Brushed DC electric motor - Wikipedia, the free encyclopedia en.wikipedia.org

[80] Ed Ramsden, "Hall-effect sensors: theory and applications", Elsevier 2006. ISBN 0-7506-7934-4.

[81] R. S. Popovi, "Hall Effect devices", CRC Press, 2004. ISBN 0-7503-0855-9.

[82] A. Baumgartner, "Classical Hall effect in scanning gate experiments", Phys. Rev. B 74, 2006.

[83] L. Y. Wang, G. G. Yin, and J.-F. Zhang, "System identification using quantized data," in 14th IFAC symposium on system identification, Newcastle, Australia, 2006.

[84] Y. Zhao, J. Zhang, L. Y Wang, G. G. Yin "Idintificatio Of Hammerstein Systems With Quantized Observations" , SIAM Society for Industrial and Applied Mathematics. Journal CONTROL OPTIM , 2010 Vol. 48, No. 7, pp. 4352-4376

[85] L. Y. Wang, G. G. Yin, and J.-F. Zhang, Y. Zhao, "System Identification With Quantized Observations, System and Control: Foundation and Application", Book, 2010, Part 2.

[86] Y. Da, X. Shi, M. Krishnamurthy, "Health monitoring, fault diagnosis and failure prognosis techniques for Brushless Permanent Magnet Machines," Vehicle Power and Propulsion Conference (VPPC), 2011 IEEE , vol., no., pp.1-7, 6-9 Sept. 2011.

[87] X. Liu; H. Zhang; J. Liu; J. Yang; , "Fault detection and diagnosis of permanent-magnet DC motor based on parameter estimation and neuralnetwork," Industrial Electronics, IEEE Transactions on , vol.47, no.5, Oct 2000.

[88] J. Treetrong, "Electric Motor Fault Diagnosis Based on Parameter Estimation Approach Using Genetic Algorithm", IMEC 2010, conference Hong Kong. 2010

[89] J.G. Proakis and M. Salehi, *Digital Communications*, 5th Edition, McGraw-Hill Higher Education, New York, 2008.

[90] Mohammad A Obeidat, Le Yi Wang, Feng Lin, Real-time parameter estimation of PMDC motors using quantized sensors, IEEE Transactions on Vehicular Technology, Vol. 62, Issue 6, pp. 1-10, July 2013.

[91] B.C. Kuo, *Digital Control Systems*, 2nd. Edition, Oxford University Press, Oxford, UK, 1995.

[92] Farid Golnaraghi, Benjamin C. Kuo, Automatic Control Systems, 9th edition, Wiley, July 2009.

[93] L.Y. Wang and G. Yin, Asymptotically efficient parameter estimation using quantized output observations, *Automatica*, vol. 43, pp. 1178-1191, 2007.

ABSTRACT

REAL TIME ESTIMATION, QUANTIZATION, AND REMOTE CONTROL OF PERMANENT MAGNET DC MOTORS

by

MOHAMMAD ALI OBEIDAT

December 2013

Advisor: Prof. Le Yi Wang

Major: Electrical Engineering

Degree: Doctor of Philosophy

Establishing real-time models for electric motors is of importance for capturing authentic dynamic behavior of the motors to improve control performance, enhance robustness, and support diagnosis. Quantized sensors are less expensive and remote controlled motors mandate signal quantization. Such limitations on observations introduce challenging issues in motor parameter estimation. This dissertation develops estimators for model parameters of permanent magnet direct current motors (PMDC) using quantized speed measurements. A typical linearized model structure of PMDC motors is used as a benchmark platform to demonstrate the technology, its key properties, and benefits. Convergence properties are established. Simulations and experimental studies are performed to illustrate potential applications of the technology.

Remotely-controlled Permanent Magnet DC (PMDC) motors must transmit speed measurements and receive control commands via communication channels.

Sampling, quantization, data transfer, and signal reconstruction are mandatory in such networked systems, and introduce additional dynamic subsystems that substantially affect feedback stability and performance. The intimate interaction among sampling periods, signal estimation step sizes, and feedback dynamics entails careful design considerations in such systems. This dissertation investigates the impact of these factors on PMDC motor performance, by rigorous analysis, simulation case studies, and design trade-off examination. The findings of this dissertation will be of importance in providing design guidelines for networked mobile systems, such as autonomous vehicles, mobile sensors, unmanned aerial vehicles which often use electric motors as main engines.

AUTOBIOGRAPHICAL STATEMENT

MOHAMMAD ALI OBEIDAT

Education

- Ph.D. in Electrical Engineering, December 2013
  Wayne State University, Detroit, Michigan
- M.S. in Electrical Engineering/Industrial Automation, June 2006
  Yarmouk University, Irbid, Jordan
- B.S. in Electrical Engineering, February 1999
  Jordan University Of Science And Technology, Irbid, Jordan

Awards

- Graduate Research Assistantship, Department of Electrical and Computer Engineering, Wayne State University, Fall/2013.
- Summer Dissertation Fellowship, Wayne State University, 2012.
- Thomas C. Rumble University Graduate Fellowship, Department of Electrical and Computer Science, Wayne State University,2012.
- Best Poster Award at IEEE Spring Southeastern Michigan Conference, April 2012.
- Sigma Xi, The Scientific Honor Research Society, 2012, Tau Beta Pi, Engineering Honor Society, 2012, and Golden Key Honor Society, 2011.

Selected Publications

1. Mohammad A Obeidat, L.Y. Wang, "Signal Estimation and Closed-Loop System Performance of PMDC Motors with Communication Channels". Submitted.
2. Mohammad A Obeidat, L.Y. Wang, F. Lin, R eal-Time Parameter Estimation of PMDC Motors using Quantized Sensors IEEE Transactions on Vehicular Technology, Vol. 62, Issue 6, pp. 1-10, July 2013.
3. Mohammad A Obeidat, L.Y. Wang, F. Lin, Online Parameter Estimation of PMDC Motors using Quantized Output Observations, ITEC IEEE Transportation Electrification Conference, Dearborn, Michigan, June 18-20, 2012.
4. Mohammad A Obeidat, L.Y. Wang, F. Lin, O n-Line Parameter Estimation of PMDC Motors using Binary-Valued Speed Measurements, PECI Power and Energy Conference at Illinois, University of Illinois at Urbana Champaign, Illinois, February 24-25, 2012.
5. Mohammad A Obeidat, L.Y. Wang, F. Lin, S peed Identification of PMDC Motors using Binary Sensors SEM IEEE Spring Southeastern Michigan conference, April 2012.